U.PORTO
FACULDADE DE CIÊNCIAS
UNIVERSIDADE DO PORTO

INSTITUTO
DE INVESTIGAÇÃO
E INOVAÇÃO
EM SAÚDE
UNIVERSIDADE
DO PORTO

Study of the lung immune response to group B streptococcal neonatal infection

Ana Sofia Magalhães Moreira Teixeira,
Master's Degree in Cellular and Molecular Biology
Department of Biology, FCUP
2022

Orientador
Elva Bonifácio Andrade, Researcher, Institute for Research and Innovation in Health (i3S), University of Porto

Todas as correções determinadas pelo júri, e só essas, foram efetuadas.

O Presidente do Júri,

Porto, _____/_____/_____

Agradecimentos

Após este ano de trabalho e descoberta, gostava em primeiro lugar de agradecer à Elva. Por me ter aceitado como sua aluna, pelo apoio incansável, pela boa disposição, pela emoção que tem por todas as pequenas vitórias com um otimismo irremediável que contagiam quem trabalha consigo. Obrigada por todos os ensinamentos que partilhou comigo durante este ano.

Um enorme obrigada a todas as pessoas com quem tive o prazer de contactar durante este período no I3s, aos colegas de laboratório pela ajuda que sempre ofereceram quer seja numa experiência, quer seja numa conversa que por vezes são tão precisas. Independentemente do tempo que tenham passado no nosso grupo, levo comigo um bocadinho de todos.

Aos amigos, que sempre me apoiaram e motivaram durante este percurso, obrigada pela paciência, não teria sido possível chegar aqui sem vocês.

Por fim, a minha família, o maior dos obrigadas por fazerem com que fosse possível seguir este trajeto. Obrigada pelo encorajamento e esforço para que sempre desse o melhor de mim.

Declaração de Honra

Eu, Ana Sofia Magalhães Moreira Teixeira, inscrita no Mestrado em Biologia Celular e Molecular da Faculdade de Ciências da Universidade do Porto declaro, nos termos do disposto na alínea a) do artigo 14.º do Código Ético de Conduta Académica da U.Porto, que o conteúdo da presente dissertação reflete as perspetivas, o trabalho de investigação e as minhas interpretações no momento da sua entrega.

Ao entregar esta dissertação, declaro, ainda, que a mesma é resultado do meu próprio trabalho de investigação e contém contributos que não foram utilizados previamente noutros trabalhos apresentados a esta ou outra instituição.

Mais declaro que todas as referências a outros autores respeitam escrupulosamente as regras da atribuição, encontrando-se devidamente citadas no corpo do texto e identificadas na secção de referências bibliográficas. Não são divulgados na presente dissertação quaisquer conteúdos cuja reprodução esteja vedada por direitos de autor.

Tenho consciência de que a prática de plágio e auto-plágio constitui um ilícito académico

.

Ana Sofia Magalhães Moreira Teixeira

Porto, 15 de Novembro 2022

This work was supported by National Funds through Fundação para a Ciência e a Tecnologia (FCT), under the project EXPL/SAU-INF/1217/2021.

Resumo

A bactéria estreptococos do grupo B (EGB) é a principal causa de infeções invasivas severas durante o período perinatal, incluindo a pneumonia e a septicémia. Os recém-nascidos adquirem a bactéria através da ingestão ou aspiração de fluídos contaminados, durante o nascimento, colocando o EGB em contacto com o sistema respiratório. Na realidade, o EGB é a causa mais frequente de pneumonia bacteriana adquirida durante o nascimento, levando anualmente, à morte de milhares de bebés. Apesar de vários estudos terem caraterizado a reposta imunitária neonatal à infeção por EGB, a resposta imunitária local no pulmão dos recém-nascidos permanece pouco estudada. Assim, neste estudo, visamos compreender melhor a patogenicidade da pneumonia por EGB, através da avaliação do curso de infeção e resposta imunitária neonatal no pulmão, usando um modelo de infeção por EGB em murganho estabelecido pelo nosso grupo.

Com este objetivo, fêmeas de murganho C57BL/6 foram inoculadas intravaginalmente (i.vag) com uma estirpe hiper virulenta de EGB, ou PBS, no décimo sexto e décimo sétimo dia de gestação. A sobrevivência, ganho de peso e colonização dos recém-nascidos foram analisadas nos dias pós-natal (P) 1, 3 e 5. Os resultados obtidos revelaram uma elevada colonização nos dias P1 e P3. Verificou-se ainda uma percentagem de mortalidade de aproximadamente 58% e uma diminuição do peso nos primeiros 5 dias de vida dos murganhos. Para além disto, a avaliação histopatológica revelou lesões nos pulmões dos animais infetados consistentes com pneumonia. Com o propósito de melhor caracterizar a resposta imunitária local, a frequência e número da população de células mieloides e linfoides foi estudada através da citometria de fluxo, nos animais não infetados e infetados. Os resultados mostram um recrutamento eficiente de neutrófilos em recém-nascidos. As células T γδ também se encontram aumentadas nos animais infetados. A infeção bacteriana perinatal induziu, em particular, a acumulação de células T γδ produtoras da interleucina 17A (IL-17A), uma citocina que conduz ao recrutamento de neutrófilos. Uma vez que as células T γδ estão também associadas com à homeostasia do pulmão, reparação de tecido e manutenção da integridade da barreira, estudamos estas células num dia posnatal mais tardio (P15). Apesar de não se terem observado diferenças no número total de células T γδ entre grupos, uma percentagem significativa apresenta um perfil consistente com residência nos animais infetados. Isto não foi observado nas células do baço em animais sobreviventes à infeção. A avaliação histopatológica do pulmão nesta idade revelou que

animais infetados apresentam maiores áreas de tecido com alterações comparando com animais não infetados.

Estes resultados levaram-nos a colocar a hipótese de que as células T γδ produtoras de IL-17A proporcionam uma primeira linha de defesa contra pneumonia por EGB. Contudo, ao usar um murganho geneticamente modificado, sem células T γδ, TCRδ$^{-/-}$, não encontramos um papel protetor destas células durante a fase aguda da infeção por EGB, uma vez que não foram encontradas diferenças na percentagem de sobrevivência ou na colonização bacterial entre o pulmão de recém-nascidos TCRδ$^{-/-}$ e a estirpe selvagem.

Para compreender o que pode estar a levar a morte dos recém-nascidos, estes foram estratificados por severidade da doença. Os resultados mostram que a severidade da doença está associada com uma maior colonização bacteriana do pulmão neonatal. Interessantemente, não se observaram diferenças na população de neutrófilos entre doença por EGB moderada e severa, estando, no entanto, aumentada em comparação com os controlos não infetados. Contudo, animais com sinais de doença moderada apresentaram um aumento significativo de neutrófilos com elevada expressão do marcador SiglecF (SiglecF^{high}), o que não foi observado em animais com sinais de doença severa. Mostramos ainda que estes neutrófilos têm uma maior capacidade de fagocitose quando comparados com neutrófilos com níveis baixos de SiglecF. Estes resultados sugerem que estes neutrófilos são cruciais para eliminação da bactéria do pulmão de recém-nascidos. Para além disto, os nossos resultados indicam que os neutrófilos SiglecF^{high} têm origem em neutrófilos convencionais no tecido do pulmão, uma vez que os neutrófilos circulantes dos recém-nascidos com doença moderada não apresentam este fenótipo.

Adicionalmente, para compreender melhor se a severidade da doença pode resultar no aumento de inflamação no pulmão, a expressão de genes de citocinas foi avaliada por RT-qPCR, em P3. Os resultados revelaram um perfil de inflamação fraco com apenas a expressão da citocina pro-inflamatória *Il1b* a estar significativamente aumentada nos animais severos comparando com os animais controlo não infetados. A expressão de *Tnfa*, *Il33*, *Il17* e *Il10* não foi diferente entre grupos. A expressão de *Il17* apenas foi observada em animais com doença moderada. Para além disto, a análise de neuropéptidos envolvidos na regulação da resposta imunitária mostrou um aumento significativo do péptido relacionado com o gene da calcitonina (CGRP), um neuropéptido conhecido por modelar neutrófilos.

Por último, para determinar se as diferenças observadas são exclusivas do clone hiper virulento utilizado, foram feitos estudos de infeção com uma estirpe de EGB menos severa (NEM316). Como esperado, a estirpe NEM316 apresenta traços menos virulentos quando comparada com a estirpe hiper virulenta, com recém-nascidos a apresenta uma maior sobrevivência e cargas bacterianas mais baixas no pulmão. Apesar desta estirpe ter sido menos eficiente no recrutamento de neutrófilos para o local de infeção, verificou-se que estes apresentam um aumento do perfil SiglecF^{high}. Estes animais também não apresentaram alterações relativamente à expressão de *Cgrp*, *Il6* e *Il10*, comparando com o grupo os animais não infetados.

Em conclusão, nesta dissertação, mostramos que pneumonia neonatal severa por EGB não está relacionada com um ineficaz recrutamento de neutrófilos para o local de infeção, mas sim com a ativação do perfil dessa célula efetora. Em acréscimo, os nossos dados preliminares oferecem nova informação numa possível modulação do eixo neuro-imune usado pelo EGB para evadir o sistema imunológico do hospedeiro.

Palavras-chave: Estreptococos do grupo B*;* infeção; imunidade neonatal; pneumonia; pulmão; neutrófilo; SiglecF; neuropéptidos; CGRP

Abstract

Group B *Streptococcus* (GBS) is the leading cause of severe invasive neonatal infections worldwide, including pneumonia and septicaemia. Neonates acquire the bacteria through ingestion or aspiration of contaminated fluids, during birth, placing GBS in close contact with the respiratory system. Indeed, GBS is the most frequent cause of bacterial pneumonia acquired at birth, leading to the death of thousands of infants annually. Although several studies have characterised the neonatal immune response to GBS, the local immunity in the neonatal lung remains to be elucidated. Therefore, in this study, we aim to better understand the GBS pneumonia pathogenesis, by evaluating the course of infection and the neonatal lung immune response, using a clinically relevant mouse model of GBS infection established by our group.

For that purpose, C57BL/6 pregnant mice were inoculated with a hypervirulent strain of GBS, or PBS, intravaginally (i.vag.) at gestational day 16 and 17. Pups survival, weight gain, and lung colonisation were analysed at postnatal day (P) 1, 3 and 5. The obtained results revealed a high and detectable colonisation at P1 and P3. A percentage of mortality of approximately 58% and a decrease in weight gain were also verified in the first five days of life. Furthermore, the histopathologic evaluation of the lungs revealed lesions in the infected animals that are consistent with pneumonia. To characterise the local immune response, the frequency and number of myeloid and lymphoid cell populations were studied by flow cytometry in the lung of infected and uninfected animals. Results show efficient recruitment of neutrophils in infected pups. The γδ T cells were also found increased in infected pups. Particularly, neonatal bacterial infection induced the accumulation of interleukin-17A (IL-17A)-producing γδ T cells, a cytokine that drives neutrophil recruitment. Furthermore, as γδ T cells are also associated with lung homeostasis, tissue repair, and maintenance of barrier integrity, we studied them at a later time point (P15). Although no differences were observed in the total number of γδ T cells between groups, a profile consistent with residency was found increased in infected pups. This was not observed in splenic γδ T cells. Histopathologic evaluation of the lung at this time point reveal that infected animals presented larger areas of tissue with alterations comparing to uninfected controls.

These results led us to hypothesise that IL-17-producing γδ T cells provide a first line of defence against GBS pneumonia. However, using genetic modified mice, that lack γδ T cells, we found no protective role of these cells during the acute phase of GBS infection as no differences were found in the percentage of survival or bacterial colonisation in the lung between TCRδ$^{-/-}$ and wild-type pups.

To understand what could be leading to neonatal death, infected newborns were stratified by disease severity and analysed. The results show that disease severity is associated with higher bacterial colonisation in the neonatal lung. Interestingly, no differences were observed in the neutrophil population between pups with moderate or severe GBS disease, being both groups significantly increased compared to uninfected controls. However, pups with moderate signs of disease show a significant increase of SiglecF^{high} neutrophils, which was not observed in pups with severe disease. We further show that SiglecF^{high} neutrophils have higher phagocytic ability when compared to the SiglecF$^{neg/low}$ counterparts, suggesting that they are crucial for bacterial clearance in the neonatal lung. Moreover, our results suggest that SiglecF^{high} neutrophils are derived from conventional neutrophils in the lung tissue, as circulating neutrophils from pups with moderate disease did not have this phenotype.

To better understand if disease severity could result from increased inflammation in the lung, the cytokine gene expression was evaluated by RT-qPCR, at P3. The results revealed a weak profile of inflammation with a significant increase in gene expression only in the pro-inflammatory cytokine *Il1b* in severe animals as compared to uninfected controls. The expression of *Tnfa*, *Il33*, *Il17* and *Il10* was not different between groups. The expression of *Il17* was only observed in pups with moderate disease. Moreover, analyses of neuropeptides involved in immune regulation show a significant increase in calcitonin gene-related peptide (CGRP) relative expression in pups with severe disease, a neuropeptide known to modulate neutrophils.

Finally, to determine whether the observed differences are exclusive of a hypervirulent clone we performed infection studies using a less severe GBS strain (NEM316). As expected, the NEM316 strain presents less virulent traits than the hypervirulent isolate, with pups presenting increased survival and lower bacterial loads in the lung. Although this strain was less efficient in the recruitment of neutrophils to the site of infection, they were found to have an increase in the SiglecF^{high} profile. These animals also do not have altered relative gene expression of *Cgrp*, *Il1b,* and *Il10*, compared with the uninfected group.

In conclusion, in this dissertation, we show that severe neonatal GBS pneumonia does not affect the recruitment of neutrophils to the site of infection, but rather their cell activation profile. Moreover, our preliminary data offers new insights in a possible modulation of the neuro-immune axis used by GBS to evade the host immune system.

Keywords: Group B *Streptococcus*; infection; neonatal immunity; pneumonia; lung; neutrophil; SiglecF; neuropeptide; CGRP

Index

List of Tables

List of Figures

Abbreviations List

A

ACK – Ammonium Chloride Potassium

AIM – absent in melanoma

ALR – AIM-like receptors

AMP – antimicrobial peptide

APC – antigen presenting cells

ARDS – Acute respiratory distress syndrome

AREG – amphiregulin

B

BFA – Brefeldin A

C

CC – Clonal complex

CD – Cluster of differentiation

cDC – conventional dendritic cell

cDNA – Complementary DNA

CFU – Colony forming units

CGRP – calcitonin gene related peptide

CLR – C-type lectin receptors

CPS – Capsular polysaccharide

D

DAMPs – damage associated molecular patterns

DC – dendritic cells

DEPC – diethyl pyrocarbonate

DNA – deoxyribonucleic acid

DPBS – Dulbecco's Phosphate Buffered Saline

E

EDTA –Ethylene diamine tetraacetic acid

e.g. – Exempli gratia

ELISA – Enzyme-linked immunosorbent assay

EOD – Early-onset disease

F

FACS – Fluorescence activated cell sorting

FBS – fetal bovine serum

FGP – fibroblast growth factor

FMO – Fluorescence minus one

FVD – fixable viability dye

Fwd – forward

G

G – Gestation

GBS – Group B *Streptococcus*

G-CSF – granulocyte colony-stimulating factor

H

h – hours

H&E – Hematoxylin and Eosin

HPRT – hypoxanthine phosphoribosyltransferase

HSC – hematopoietic stem cells

HylB – Hyaluronidase

I

I3S – Instituto de Investigação e Inovação em Saúde

IAP – intrapartum antibiotic prophylaxis

IL – Interleukin

IFN – Interferon

i.vag – intravaginally

J

K

KC – keratinocyte

L

LOD – Late-onset disease

M

MFI – mean fluorescence intensity

MHC – major histocompatibility co plex

min – minutes

MIP – macrophage inflammatory protein

miR – microRNA

MOI – multiplicity of infection

MPO – myeloperoxidase

mRNA – messenger RNA

N

NET – neutrophil extracellular traps

NK – natural killer cell

NLR – NOD-like receptors

NMU – neuromedin U

NOD – nucleotide oligomerization domain

O

OD – optical density

o.n. – overnight

P

P – postnatal day

PAMPs – pathogen-associated molecular patterns

PBP1a – Penicillin binding protein

PBS – Phosphate-buffered saline

pDC – plasmacytoid dendritic cell

PMA – Phorbol 12-Myristate 13-Acetate

PROM – prelabour rupture of membranes

PRR – pattern recognition receptor

Q

R

Rev – reverse

RIG – Retinoic acid-inducible gene

RLR – RIG-I-like receptors

RNA – Ribonucleic acid

ROS – reactive oxygen species

RT – room temperature

RT–qPCR – Real-time Polymerase Chain Reaction

S

s – seconds

SEM – standard means

SiglecF – sialic acid–binding immunoglobulin-like lectin F

SP – surfactant protein

SPLUNC – short palate lung and nasal epithelium clone 1

SR – scavenger receptors

Srr – Serine rich repeat

T

TA – Temperature of annealing

TCR – T cell receptor

TH – Todd-Hewitt

Th – T helper cell

TLR – Toll-like receptor

TNF – tumour necrosis factor

U

V

Vip – vasoactive intestinal peptide

W

X

Y

Z

ß

ß-h/c – ß -hemolysin/cytolisin

Introduction

1.1. Group B *Streptococcus*

Group B *Streptococcus* (GBS), or *Streptococcus agalactiae*, is an anaerobic aerotolerant, Gram-positive diplococcus bacteria which causes severe neonatal disease and mortality. GBS is a commensal organism of the gastrointestinal and vaginal tracts of healthy adults when limited to the mucous membrane. The gastrointestinal tract acts as the reservoir of GBS and a source for colonisation of the genitourinary tract in an intermittent, transitory, or persistent manner (1-3). Nevertheless, GBS can become infectious and cause invasive diseases in neonates, postpartum women, and nonpregnant adults with underlying medical conditions, such as immunosuppression (4-6).

In fact, in neonates, GBS is the leading cause of life-threatening bacterial infections (4). Invasive neonatal GBS disease has an estimated worldwide incidence of 0.49 per 1000 live births (7). Importantly GBS is estimated to cause the death of 90,000 infants and 57,000 stillbirths annually (8). Several obstetrical risk factors contributing to heighten the neonatal risk for developing invasive disease exist, including vaginal and/or rectal colonisation during pregnancy (9, 10), along with colonisation on a previous pregnancy (1, 2), maternal age (11), intraamniotic infection (1), low birth weight (12, 13), preterm delivery (9, 11), intrapartum maternal fever, and prelabour rupture of membranes (PROM) (1, 9).

Most GBS isolates can be classified into ten serotypes (Ia, Ib, II to IX) based on the expression of specific antigens of an important virulent factor, the sialic acid-rich capsular polysaccharide (CPS) (9, 14, 15). When the CPS cannot be identified, the isolate is deemed to be nontippable (16). GBS strains can be further grouped into clonal complexes (CC), based on the allelic variation of seven housekeeping genes (17). However, the invasive nature of GBS comes not only from the expression of CPS but from a wide range of other important virulence factors that favour its dissemination and pathogenesis, such as GBS hyaluronidase (HylB) that targets and degrades a component of the host extracellular matrix, the hyaluronic acid (10); GBS serine-rich repeat glycoproteins (GBS srr), that binds to host epithelial cells (15); GBS extracellular protein BsaB, that interacts with the epithelium leading to increased adherence and thus promoting maternal colonisation and proliferation (10, 15); the surface localized protease, C5a peptidase, which interferes with the complement mediated chemoattraction of neutrophils, as C5a is an important unit of this mechanism, and

therefore protecting from phagocytosis (15, 18); the penicillin-binding protein (PBP1a) that increases resistance to neutrophil killing (19); GBS alpha C protein, that binds to the cell surface and promotes internalization of GBS on cervical epithelial cells (20, 21); and the pore-forming toxin β-hemolysin/cytolysin (β-h/c) that improves dissemination and supports severe disease in newborns (22, 23).

Furthermore, GBS infection was shown to alter the expression of microRNAs (miR), a group of small non-coding RNAs that regulate gene expression at the post-transcriptional level, such as the miR-155-5p, in *Macaca nemestrina*, which can act as a biomarker of lung injury, in addition, to altering the expression of fibroblast growth factor 9 (FGP9) leading to aberrant lung development (24). In a murine model of GBS-induced pneumonia, GBS was also found to increase the expression of miR-223, essential for the control of neutrophils proliferation and activation (25), which in turn led to the down-regulation of inflammatory cytokines, such as interleukin-1β (IL-1β) and tumour necrosis factor-α (TNF-α) (26).

1.2. Preventing neonatal infections - current treatment

Despite the efforts to produce a maternal vaccine that would provide active immunization to the mother and passive protection of the neonate (18, 27, 28), based on the more common GBS serotypes associated with neonatal disease, namely serotype Ia, Ib, II, III, IV, and V solely or conjugated with GBS surface proteins (2, 3, 27), there is no commercially available vaccine to prevent GBS infections. The current strategy to reduce the risk of GBS disease is based on antenatal screening to detect vaginal and/or rectal carriage of GBS and intrapartum antibiotic prophylaxis (IAP). IAP consists of administering antibiotics to the pregnant woman 4 hours (h) before birth for maximum effectiveness. However, it is necessary to control the administration of IAP so there are no unnecessary antibiotics given to people that do not require it, as it might lead to GBS antibiotic resistance, as it has been observed in the sensitivity to clindamycin and erythromycin, or even further the disruption of the gastrointestinal microbiota (2, 27, 29, 30). Therefore, to determine which woman receives this treatment, a set of steps are usually followed: first a collection of material in the vaginal-rectal zone followed by cultures and processing to identify the presence of GBS. This type of screening is usually made between 36 and 37 weeks of gestation (1, 2), and all the women that reveal to be positive for GBS are recommended for IAP. This strategy is not recommended in caesarean birth as long as there is not rupture of membranes (1, 2).

Penicillin G is the antibiotic of choice for IAP because it has a more targeted spectrum of antimicrobial activity against Gram-positive bacteria. However, for people

allergic to penicillin other antibiotics must be taken into consideration, such as cefazolin (first-generation cephalosporin), or if there is also susceptibility to cefazolin, clindamycin, or vancomycin (1).

Furthermore, upon birth, rapid detection of infection and appropriate treatment is imperative as GBS infection can become life-threatening. When the birth occurs at ≥ 35 weeks of gestation, the risk of infection can be assessed by three different methods: categorical risk assessment, multivariate risk assessment, and risk assessment based on the clinical signs from the newborn. These three types of assessment take into account several factors in order to provide the best follow-up and care to neonates, such as the presence of clinical signs of illness, the adequate or inadequate administration of IAP, and maternal intrapartum temperature. Based on the risk assessed, the newborn can receive routine care, be placed into clinical observation for a period of 36 to 48 h and/or be submitted to treatment with the antibiotics together with the performance of blood cultures (31). If the infant is born with < 35 weeks of gestation, other factors must be taken into count to classify the newborns risk of GBS infection, such as the conditions that lead to the premature birth, if the PROM and/or if signals of intraamniotic infection are present (31).

Upon infection diagnosis, by isolation of the bacteria from usually sterile sites with respiratory complications, such as pneumonia, exogenous surfactants are usually used as a treatment. Natural lung surfactant is constituted of a mixture of proteins and complex phospholipids that delineates and keeps alveoli free of fluid while reducing alveolar surface tension (32, 33).

1.3. GBS neonatal disease

1.3.1. GBS early-onset disease

Two different syndromes of invasive GBS disease can result from neonatal infection and are classified by age at onset. The GBS early-onset disease (EOD) presents itself within a period of 12-48 h until seven days after birth and is characterized by respiratory distress, followed by septicaemia, pneumonia and, more rarely, meningitis (1, 2, 9, 10). In this syndrome, the bacteria are most probably acquired by vertical transmission from the mother to the newborn by aspiration of contaminated amniotic fluid before delivery, due to the ascension of bacteria from the vaginal mucosa to the utero and passage through intact membranes, or by aspiration and/or ingestion of vaginal secretions during delivery (1, 2, 10, 30). In recent years the overall incidence of GBS EOD has decreased due to the use of IAP. However, this syndrome is still particularly

problematic in preterm neonates as they are associated with a higher incidence of GBS EOD and a higher mortality rate in comparison to term neonates (27, 31).

The primary organ of the newborn affected by the invasion of GBS is the lung, as GBS is placed in close contact with pulmonary cells considering that the respiratory system presents an interface with the environment. This leads to inflammation and respiratory complications after birth as a result of lung injuries (1, 24, 33). The initial clinical findings of GBS disease in all infants are acute respiratory signs that mostly lead to pneumonia which can then progress to acute respiratory distress syndrome (ARDS), causing severe acute lung injury and hypoxemia (34-36). In fact, GBS is pointed as the most frequent cause of bacterial pneumonia acquired at delivery and data from fatal cases demonstrates that a large portion of the infants has evidence of lobar or multilobar pneumonia (37-39).

1.3.2. GBS late-onset disease

The second syndrome resulting from invasive GBS infection is the late-onset disease (LOD). In this syndrome, symptoms are present from the seventh day upon birth until the newborn reaches 90 days, and it manifests more commonly as bacteraemia without focus and meningitis. The presence of nonspecific signs, such as fever, irritability, and poor feeding, makes diagnosing an infant with LOD very difficult. Importantly, LOD is associated with increased mortality and neurocognitive impairment ranging from mild to severe impairment (11, 27, 40, 41). Currently, this syndrome presents a higher incidence in newborns than GBS EOD, as a result from the implementation of IAP that reduced the incidence of GBS EOD. However, this preventive strategy had no effect on the incidence of GBS LOD (2, 30, 42, 43).

The form of acquisition of LOD is not yet fully characterized but is believed to be mainly by horizontal transmission through environmental or community sources, especially in preterm neonates that are required to stay in neonatal intensive care unit for extended periods of time (1, 9, 12). Nevertheless, vertical transmission cannot be excluded.

1.4. Innate immunity

Immune cells are mainly divided into two classes, the myeloid cells and the lymphoid cells, although their share a common precursor, the hematopoietic stem cell (HSC) in the bone marrow. HSC will then differentiate in multipotent progenitor cells that will later commit to a cell lineage. Myeloid cells comprise most of the innate immune cells, such as monocytes that differentiate in macrophages upon migration to infected sites, and a big part of the dendritic cells (DC) and granulocytes that differentiate in

basophils, eosinophils, and neutrophils. As for the lymphoid lineage, their cell program is more directed toward adaptative immunity, with all of the lymphocytes included in this cell lineage (44, 45).

The innate immune system can be defined as a group of protective measures that are always present and react rapidly upon external aggression. This system has as the first line of defence epithelial surfaces, which form a physical barrier between the environment and the host tissue. At the same time epithelial surfaces also provide protection against microbes by producing antimicrobial peptides, such as defensins, cathelicidins and histatins (46). When microbes breach these defences, cells of the innate immune system, such as macrophages and DC, detect their presence and phagocytosis is initiated. Activation of phagocytic cells, along with other tissue resident cells leads to the production and release of pro-inflammatory cytokines, interferons and chemokines that are responsible for the recruitment of neutrophils, macrophages, natural killer (NK) cells and later lymphocytes into the injured site with the objective of containing the infection by killing the invasive agent and disposing of damaged host cells in a complex process called inflammation (47). Constitutively expressed molecules, such as complement, add additional molecular mechanisms that act as first line of defence against invading pathogens (48).

The innate immune system cells recognise microbes by recognising pathogen-associated molecular patterns (PAMPs), conserved molecules produced by microbes that are essential for their survival. The recognition of damage associated molecular patterns (DAMPs), which are molecules produced and released by damaged infected cells also activates the innate immune system and is frequently a signal of infection. These recognition mechanisms allow the recognition of large groups of pathogens but never the recognition of a specific agent or antigen (49).

PAMPs and DAMPs are recognized by germline-encoded pattern-recognition receptors (PRRs) that are present both intra and extracellularly. PRRs are divided into two classes. The class of the receptors bounded to membranes, namely C-type lectin receptors (CLRs), that are bounded to the cell surface and Toll-like receptors (TLRs) that are bound either to cell surface or endocytic compartments. The class of intracellular and unbounded receptors, specifically retinoic acid-inducible gene I (RIG)-like receptors (RLRs), nucleotide oligomerization domain-like (NOD-like) receptors (NLRs) and absent in melanoma 2 (AIM2)-like receptors (ALRs), (Figure 1). This type of receptors distribution is what allows the recognition microbes in different cellular locations (49-51).

Additionally, scavenger receptors (SR) a superfamily of proteins, can be found either anchored to the extracellular membrane or secreted (52) .

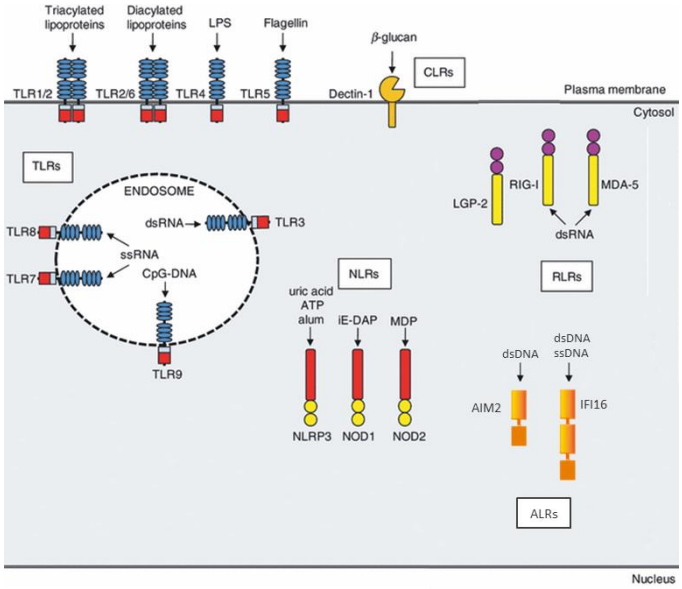

Figure 1. Schematic representation of cellular localization of the pattern-recognition receptors (PRRs) and respective ligands. C-type lectin receptors (CLRs) are located in the cell surface. Toll-like receptors (TLRs) era located both in the cells surface and the membrane of the endosome. Retinoic acid-inducible gene I – like receptors (RLRs), nucleotide oligomerization domain-like (NOD-like) receptors (NLRs) and absent in melanoma 2 (AIM2)-like receptors (ALRs) are present in the cytoplasm. Adapted from (53, 54)

1.4.1 Neonatal immunity and innate immune cells

Newborns are particularly vulnerable to infectious agents because they are still developing their immune system. Also, they have little immunological memory, which makes them rely on their innate immune response for protection (55). Yet, the innate immune system from neonates is tightly regulated and biased towards an anti-inflammatory state, with decreased production of pro-inflammatory cytokines (ex. TNF-α, IL-1β) and increase in anti-inflammatory cytokines (ex. IL-10) (55). This tight regulation exists to prevent excessive inflammatory reactions that could cause harm to the animal (56).

Neutrophils are a population of innate cells that is highly enriched in the blood. When an infection occurs, these cells rapidly migrate to the site of infection where they can survive for 1 to 4 days. Unfortunately, despite the neonates having a higher number of neutrophils at birth, the migration process is diminished (55, 57-59). The main mechanism of action of the neutrophil is the phagocytose of microbes, leading to the production of reactive oxygen species (ROS) (58, 60). The neutrophil can also incur in neutrophil degranulation in which the proteins of the granule known for having antimicrobial effect are released, and the production of ROS is also activated. Finally, the neutrophil can form neutrophil extracellular traps (NETs), composed of extruded DNA

that is associated with antimicrobial neutrophil granule proteins, that bind to microbes leading to their destruction and inhibiting their dissemination (58, 60, 61). However, in the neonate neutrophil, both the capacity for phagocytosis and the formation of NETs is reduced/defective, which has been pointed as one of the main reasons for neonatal higher susceptible to infections (55, 58). Apart from the phagocytic role, neutrophils produce inflammatory factors such as cytokines that create a crosstalk with other innate immune cells leading to the recruitment of monocytes and more neutrophils, and regulation of macrophages activity (58, 62, 63).

Two other cell types that are short-lived and possess granulocytes are the basophils and the eosinophils. Contrary to the neutrophils, these cells of types represent small percentage of circulating leukocytes, and their numbers in neonates are similar to adults (47, 59, 64-68). During a typical innate immune response, these cells are early recruited to inflammatory sites, where they release cytokines and chemokines that lead to the recruitment of more immune cells. Furthermore, these cells release their granulocyte protein, mainly by degranulation. Most of the proteins have antibacterial properties, but they can also induce tissue damage or even vasodilatation. (64-69). Eosinophils in specific show a small capacity of phagocytosis, some capacity of acting as antigen presenting cells (APCs), and finally upon bacterial infection they can extruded mitochondrial DNA traps (67). In neonates the basophils have been shown to alter the function of DC in a manner that creates an imbalance between T helper (Th) 1 /Th2 immune response, with promotion of Th2 immune program (70). Th1 cells produce IL-2 and interferon-γ (IFN-γ) and have a protective response dependent of phagocytosis. The Th2 cells produce IL-4, IL-5, IL-11 and IL-13 and are directed to a phagocytic independent protective response, such as eosinophil activation (71). Indeed, it is also common in the neonatal period in response, for example, to foreign antigens or infection, the development of eosinophilia. Eosinophilia is the count of eosinophils higher than normal which appears to be a reliable indicator of sepsis (72).

Another group of cells that is important in the neonates is the neonatal APCs, to which the macrophages and DC belong (47, 55, 73). The macrophages are long-lived cells, that can be found in all organs, where they have phagocytic ability and homeostatic tissue function (47, 74). They present high heterogeneity, and plasticity, despite the restricted number of origins, with the tissue resident macrophages having specific functions and morphology, dependent of the tissue of residence, as it is the example of the alveolar macrophages. (45, 74-76). Regarding DC, their main function is the presentation of antigens to T cells in secondary lymphoid tissues. These cells engulf the pathogen in the site of infection and migrate to a lymphoid tissue where they encounter

T cells, initiating the adaptative immune response (47, 77). Furthermore, DC can be characterized in two main groups the conventional DC (cDC) and the plasmacytoid DC (pDC) (55). In neonates the monocytes and DC have an APC impair activity as they express reduced levels of molecules of major histocompatibility complex (MHC) class II. Moreover, these cells also appear in lower numbers comparing to adults and in different proportions with neonates having a ratio of pDC to cDC of 3:1 and adults 1:3. These characteristics lead to a deficient activation of antigen specific T cell responses (55).

Other explanation for the increased susceptibility of neonates to microbial infection is the altered production of cytokines in response to TLR stimulation, which possess a clear bias against cytokines that promote Th1 cells, contrary to what is found in adults (55). Another interesting fact regarding the neonatal immune system is the NK cells. These cells have their highest cell count upon birth. However, when comparing to adults these cells also have a lower cytotoxic capacity, with decreased cytoplasmatic granules. They are easily activated by cytokines and contact with DC and macrophages, but their capacity to produce IL-15, IL-12 and IFN-γ is diminished in neonates (55, 78).

Finally, the γδ T cells are a very particular group of T cells, presenting characteristics from both adaptative and innate immunity responses. In fact, γδ T cells are mostly taken as innate immune cells, as they are the first cells to be mobilized upon infection in response to cytokines, PAMPs and DAMPs (79-81). These cells are also the first T cells to develop during embryogenesis (80, 81). Upon which, they migrate to barrier tissues such as the lungs, skin epidermis, meninges, female and male reproductive tract, and intestinal tract forming a resident population leading to their definition as tissue-resident immune cells (79, 81-83).

The barrier tissues have a stable commensal community of microorganisms that shapes the local immune system and influence the resident γδ T cells. Exposure to external aggressions and invasion by pathogens, which can disturb the present commensal community, will initiate an immune response (84-86). In this scenario, the activation of the γδ T cells can occur directly by the commensal or the pathogenic microorganisms or indirectly by recognition of pro-inflammatory cytokines, receptors that bind to viral or bacterial products and stressed cells (87, 88). Upon activation γδ T cells initiate an inflammatory response by expressing the cytokines IFN-γ or/and IL-17A; promoting the recruitment of DC and help the APC-mediated adaptative immunity forming a connection between innate and adaptative responses (79, 81, 87, 88).

1.5. Host-pathogen interactions: Innate Immune response to GBS

As already discussed, GBS has the capacity to invade the mucosa epithelium and enter the tissues, namely respiratory tissues, which normally are the point of entrance and dissemination of the bacteria (20, 21, 89, 90). However, the lung epithelium is not an ecstatic barrier and the epithelial lung cells that cover most of the organ, despite the low phagocytic ability, can directly kill pathogens (91). These cells also act by secreting cytokines upon recognition of PAMPs through TLR that will recruit macrophages and neutrophils, two important phagocytic cells. The epithelium lung can also release a significant amount of antimicrobial proteins and peptides (AMPs), such as α-defensis, β-defensis, cathelicidins that are maturated in cathelicidins-LL37 and short palate lung and nasal epithelium clone 1 (SPLUNC) (91). In particular, cathelicidins-LL37 has been demonstrated to have an active role against GBS but has a decreased production at birth compared to adults (92, 93). From recognition by the epithelial lung cells to tissue invasion, GBS triggers an immune response in the host that, particularly in neonates, is translated into an innate immune response (94). The predominantly innate immune cells present in the lung tissue and, therefore, the first to interact with invasive pathogens are alveolar macrophages, neutrophils, innate lymphoid cells, lung-resident DC and NK (73, 95). These cells also express PRR triggering a cascade of responses that are characterized by the production of pro-inflammatory cytokines, leading to further cell recruitment (96-98).

Macrophages, more than phagocytic cells, are a source of the pro-inflammatory cytokines TNF-α, IL-12, IL-1β and IFN-β (97, 99, 100). Moreover, resident alveolar macrophages appear to be the main producers of group IIA phospholipase A bactericidal enzyme, known as a crucial protector during GBS systemic infection (101). During GBS infection, signalling in macrophages through the IL-1β receptor promotes the secretion of the chemokines macrophage inflammatory protein (MIP)-1α and keratinocyte (KC) that recruit neutrophils to the site of infection (97). GBS also induces the secretion of IL-1β by macrophages, DC and neutrophils (99, 102). In DC, the secretion of activated IL-1β depends on GBS β-hemolysin, which activates the NOD-like receptor family, pyrin domain containing 3 sensor (NLRP3) of the inflammasome, that ultimately activates the enzyme caspase-1 that converts the pro-IL-1β in an active cytokine (102). In neutrophils, the secretion is induced by endosomal and cytosolic signals by TLR7/9/13, a reaction that also activates caspase-1 necessary for the secretion of activated IL-1β (99). IL-1β is a strong pro-inflammatory cytokine that leads to the influx of neutrophils creating a positive feedback cycle of these powerful phagocytic cells (99). Furthermore, *in vitro* studies have shown that macrophages are a source of IFN-β upon GBS recognition

through TLR7. IFN-β signalling is important for the expression of TNF-α and IL-6, two important pro-inflammatory cytokines (100).

Another cytokine that appears to have a beneficial role in GBS infection is IL-12 since its blockage leads to an increase in the severity of sepsis. On the other hand, the increased expression of IL-12 in response to infection leads to an increased production of IFN-γ (96). The production of IFN-γ is also increased in $CD4^+$ T cells differentiated in Th1 upon GBS stimulation, these cells also produce the pro-inflammatory cytokine TNF-α and IL-2 (103).

Despite the presence of several protective mechanisms, GBS has the ability to evade the host immune response, leading to increased susceptibility to infection. Some of these mechanisms are based on the early production of anti-inflammatory cytokine IL-10 upon TLR2 signalling, which impairs neutrophil recruitment (104). Moreover, β- h/c inhibits macrophage activation, hindering their phagocytic activity and secretion of pro-inflammatory cytokine IL-12 (105). Another mechanism is the degradation of DAMP to non-stimulatory polymers (106).

As described above, during invasive disease GBS induces a strong inflammatory response that, if left untreated, develops into pneumonia - an acute inflammation of the lower respiratory tract and lung parenchyma - and even sepsis. (39, 107). To prevent this development, compensatory mechanisms are at play (26). An animal model using New Zealand white rabbits showed that infection by GBS enhances the mRNA expression of natural surfactant proteins SP-A and SP-D (33) but also increases lipid peroxidation of exogenous surfactant, impairing the therapeutic ability (32). Therefore, an administration of an exogenous surfactant combined with antioxidants showed reduced lipid peroxidation (32). The treatment presents multiple benefits for the infected animal as the surfactant improves the histological state of the lung, reduces the passage of bacteria from the lung to the bloodstream, bacterial proliferation, and lastly reduces the inflammatory response in the lungs (33).

As aforementioned, the neonatal innate immune system plays a decisive role in the protective response against GBS. However, despite progress, neonatal immunity in the lung against this pathogen remains to be elucidated. Understanding the initial neonatal immune response against this bacterial pathogen, will significantly inform fundamental and translational principles of GBS pneumonia pathogenesis repair, of high clinical interest for developing novel effective therapies.

Aims

Our group developed a clinically relevant mouse model of GBS infection that reproduces all the steps of natural infection in human newborns, including pneumonia (22). As previously referred, the lungs are the first organ of the newborns to contact with the bacteria and where the infection is first established (1, 30, 38). However, our knowledge of the protective/detrimental immune response remains largely unknown.

We aim to investigate the natural kinetic of infection in the neonatal lungs and identify the immune cells invading this organ, as well as their relationship with disease progression, using a clinically relevant mouse model of infection. To attain this, my dissertation is divided in the following specific goals:

1. Evaluate the kinetic of bacteria colonisation and histopathology in the neonatal lung.

2. Identify the major lymphoid and myeloid cells present in the neonatal lungs during GBS infection.

3. Evaluate the contribution of the lung immune cells to bacterial clearance and protection.

4. Determine the expression of cytokines in the neonatal lungs during GBS disease.

Material and Methods

2.1. Animals and ethics statement

All experiments were conducted in mice from C57BL/6 background, either WT or TCR$\delta^{-/-}$. Mice were bred in SPF conditions and maintained under the SPF facility of the Instituto de Investigação e Inovação em Saúde (i3S), Universidade do Porto. Mice were kept under a 12 h alternating cycle of light/dark. All animal procedures were conducted following the recommendations of the European Convention for the Protection of Vertebrate Animals used for Experimental and Other Scientific Purposes (ETS 123) and Directive 2010/63/EU and Portuguese rules (DL 113/ 2013). The project was reviewed and approved by the Ethics Committee of the i3S, and by the Portuguese National Entity Direção Geral de Alimentação e Veterinária. The PI is FELASA C certified.

2.2. Bacterial strains and cultures

GBS strain BM110, belonging to the hypervirulent CC 17 (108, 109), or the GBS strain NEM316 belonging to the CC23 (17, 110) was cultured overnight (o.n.) in liquid Todd-Hewitt (TH) medium for a maximum of 15 h. The overnight culture was then subcultured 1:100 and grown until the mid-log phase corresponding to an OD_{600} (optical density) $\approx$ 0.800. At this point the bacterial culture was centrifuged at 4000 rpm (rotations per minute), at room temperature (RT), for 7 minutes (min) creating a pellet and the medium was discarded. The pellet was washed twice with a volume of phosphate-buffered saline (PBS) equal to the discarded volume of medium and in the same conditions of centrifugation. Bacteria were suspended in PBS to an OD_{600} of $\approx$0.600 (two independent measurements were made with values between 0.595-0.605 accepted as valid), corresponding to a concentration of $2x10^8$ colony-forming units (CFU)/mL. To prepare the inoculum for mouse infection, the suspension was further diluted to $2x10^6$ CFU/mL.

To evaluate the real number of CFU given to the female mice serial dilutions from the inoculum were made and 10 µL of each was plated in TH agar, incubated o.n. at 37 °C and the CFU counted.

2.3. Neonatal Mouse Model of GBS pneumonia

In the mouse model of infection for human neonatal GBS disease, pregnant C57BL/6 and homozygotic TCR$\delta^{-/-}$ mice were inoculated intravaginally (i.vag.) with 40 µL of the inoculum containing approximately $8x10^4$ CFU of GBS at the gestation (G) days 16 and 17. The females delivered spontaneously between G19 and G20, and the pups were maintained with their mothers during the experimental time. The day following to

the birth is considered the postnatal day (P) 1. All experiments were controlled with age-matched mice born from PBS sham progenitors.

2.4. Survival Curves and Weight gain evaluation

The animals born from sham and infected pregnant mice were followed until P5 to monitor their survival curves. The pups weights were also registered until P5.

2.5. Organ harvesting

Pups (both male and female), selected at different time points as indicated in the text, were deeply anaesthetized by isoflurane inhalation, perfused with saline, and euthanized by decapitation. The lungs and spleen were aseptically removed and handled in agreement with its final use. In the case of RNA analysis, samples were snap frozen and stored at -80 °C until extraction. When needed, blood was drawn from the mandibular vein using heparin-coated capillaries prior perfusion.

2.6. Lung Colonisation evaluation

At specific time points (from P1 to P5) the collected lung was homogenized in 250 µL of PBS with a pellet pestle and a rotor-stator homogenizer. Following homogenization, serial dilutions were made in sterile PBS and 10 µL of each dilution was plated in TH agar and incubated o.n. at 37 °C for CFU enumeration.

2.7. Lung Histopathology

From each pup, at different ages as indicated in the text, the left lobe was excised and fixed in 10 % buffered formalin. Samples were routinely processed in the *TP10120* (Leica®, Wetzlar, Germany) and embedded in paraffin. For staining 3 µm thick sections were cut using the microtome Histocore Autocut (Leica®) and stained with Hematoxylin and Eosin (H&E) or Giemsa, following standard protocols. The slides were digitalized using the *Pannoramic MIDI II* (3DHISTECH, Budapeste, Hungria), with amplification of 40x and visualized using the software CaseViewer (3DHISTECH).

2.7.1. Histologic lung scores

To study the pulmonary alterations induced by infection, tissue histopathologic histology was semi-quantitatively analysed, as previously described (111). For analysis, through H&E sections, pathological features were scored using the scale parameters present in Table 1 in a blinded fashion by pathologists (Bárbara Carvalho and Joana Santos).

Table 1. Histological score established for the evaluation of pulmonary alterations

Score	Description
0	Absence of histological changes
1	Parenchymal alterations in 1 to 25 % of the tissue examined
2	Parenchymal alterations in 26 to 50 % of the tissue examined
3	Parenchymal alterations in 51 to 75 % of the tissue examined
4	Parenchymal alterations in 76 to 100 % of the tissue examined

2.8. RNA extraction with phase separation

RNA extraction was made using the Pure link™ RNA Mini Kit (Ambion by life technologies) with no DNase treatment. The protocol from the kit was followed with few alterations to the tissue homogenization point. The lung samples were homogenized in 250 µL of Trizol, volume used as all samples weighted less than 30 mg, using a rotor-stator homogenizer and pestles. Upon dissociation 750 µL of Trizol were added to complete a final volume of 1 mL. At this point the samples were transfer into ice and kept in it for the possible time as the homogenates were passed first ten times through a 25G needle and secondly ten times through a 27G needle. This was followed by an incubation for 5 min at RT, to allow the complete dissociation of nucleoprotein complexes. At the end of the incubation time, 200 µL of chloroform for each mL of Trizol was added, the samples were shaken by hand for 15 seconds (s) and incubated at RT for 2-3 min. Next, a centrifugation for 15 min at 12000 g at 4 °C, on a pre-refrigerated centrifuge, was made, resulting in the separations of two phases. The aqueous phase (colorless) was carefully removed using a micropipette, so the interface between the phases is not disrupted, to an RNase-free tube. Up this point forward the protocol from the kit was followed starting at the section of Bind RNA. The RNA was eluted in 30 µL of RNAse free water. RNA quality was evaluated using Experion™ Eukaryote Total RNA StdSens and RNA concentration was determined using a UV-Vis spectrophotometer, the Nanodrop 1000. The extracted RNA was stored at -80 °C until use.

2.9. cDNA synthesis

RNA was reverse transcribed into cDNA was using the SuperScript™ IV First-Strand Synthesis System (Invitrogen by ThermoFisher). 1 µg of RNA was used as template and 50 µM Oligo $d(T)_{20}$ primer as primer annealing. As alteration to the protocol only 0.5 µL of SuperScript™ IV Reverse Transcriptase per reaction tube was used. As control SuperScript™ IV Reverse Transcriptase was substituted by diethyl pyrocarbonate (DEPC)-treated water in an extra reaction tube. cDNA synthesized was stored at -20 °C.

2.10. Quantitative real time polymerase chain reaction (RT-qPCR)

To evaluate gene level expression RT-qPCR was performed. For this reaction each well was composed of iTaq Universal SYBR Green Supermix (Bio-Rad) (1X), specific primers (0.5 µM each primer) (Table 2), nuclease- free water and 1 µL cDNA at 1:5 of the stock concentration, to a total of 10 µL per well. For each sample a duplicate was made on the PCR plate and two negative controls were added by gene: a control where cDNA was replaced by water to evaluate the existence of contaminations and a control with the cDNA reaction where SuperScript™ IV Reverse Transcriptase was substituted by DEPC-treated water to evaluate any genomic DNA contamination. After all the components and the cDNA were added to the wells, the plate was sealed and briefly centrifuged. The PCR program used was the following:

a. 95.0 °C for 3:30 min
b. 95.0 °C for 0:20 min
c. Temperature of annealing (TA) defined for 0:20 min
d. Repeat b. and c. x39
e. Melt curve 55.0 to 95.0 °C, with an increment of 0.5 °C for 0:10 min

Relative gene expression levels were normalized to *Hprt* using the $2^{-\Delta Ct}$ method.

Table 2. Primer list with sequence and temperature of annealing

Name	Sequence (5' → 3')	TA
Areg	Fwd: GCAGATACATCGAGAACCTGG Rv: CTGCAATCTTGGATAGGTCCT	60 °C
Il1b	Fwd: CAACCAACAAGTGATATTCTCCATG Rv: GATCCACACTCTCCAGCTGCA	60 °C
Vip	Fwd: TGTGCTGTTCTCTCAGTCGC Rv: AAACGGCATCCTGTCATCCA	60 °C
Cgrp	Fwd: CCTGCAACACTGCCACCTGCG Rv: GAAGGCTTCAGAGCCCACATTG	60 °C
Il33	Fwd: TCCAACTCCAAGATTTCCCCG Rv: CATGCAGTAGACATGGCAGAA	60 °C
Nmu	Fwd: GTCCTCTGTTGTGCATCCGTT Rv: GCGTGGCCTGAATAAAAAGTA	60 °C
Hprt	Fwd: TCAGTCAACGGGGGACATAAA Rv: GGGGCTGTACTGCTTAACCAG	58/60 °C
Tnfa	Fwd:GTGGAACTGGCAGAAGAG Rv: ATGAGAAGAGGCTGAGACA	60 °C

Il17	Fwd: CTCAGACTACCTCAACCGTTCCA Rv: TTCCCTCCGCATTGACACA	58 °C
Il10	Fwd: ATTTGAATTCCCTGGGTGAGAAG Rv: CACAGGGGAGAAATCGATGACA	58 °C

2.11. Cells Isolation

2.11.1. Lung

In order to isolate the lung cells, the collected lung tissue was immediately minced and placed in a 6-well plate and digested with 2 mL of RPMI 1640 (HyClone™) with 1 mg/mL collagenase-D (Roche) at 37 ºC for 30 min. The reaction was stopped with 1 mL of PBE (2mM EDTA; 0,5% Bovine Serum Albumin; PBS). The cell mix was passed firstly through a 20G needle, followed by a 25G, five times in each needle. The suspension was then filtered through a 100 µm cell strainer and transferred to a 15 mL tube. Suspensions were centrifuged twice at 70 g for 1 min, at 4 °C, and the supernatant collected. Finally, cells were centrifuged at 300 g, for 4 min at 4 °C, and the supernatant discarded. Red blood cells were lysed with 0,5 mL of Ammonium-Chloride-Potassium (ACK) lyse buffer, washed and resuspended in 100 µL of fluorescence activated cell sorting (FACS) Buffer [2mM EDTA; 25mM HEPES; 2% fetal bovine serum (FBS), 0,01% NaN_3; Dulbecco′s PBS (DPBS)] for flow cytometry or in Sorting buffer (1mM EDTA; 25mM HEPES; 2% FBS; DPBS) for cell sorting. In the case of intracellular staining, cells were resuspended in complete RPMI 1640 medium (RPMI 1640, L-Glutamine, 10% foetal bovine serum, 1% of HEPES and 1% of penicillin and streptomycin).

2.11.2. Spleen

Upon collection the spleen was placed on 5 mL of RPMI 1640 with 2% FBS. The organ was softly dissociated and passed through a 100 µm cell strainer with a sterile plastic plunger. Cell suspension was centrifuged for 5 min at 500 g, at 4°C. After discarding the supernatant, cell pellets were resuspended in FACS buffer.

2.12. Flow Cytometry and Cell Sorting

Isolated cells were counted using trypan blue and Kova slides and a total of $1x10^6$ cells were placed in 96-well plate for staining. For intracellular staining, cells were further stimulated in complete RPMI medium with PMA (Phorbol 12-Myristate 13-Acetate; 50 ng/ml, Sigma-Aldrich) and Ionomycin (1 µg/mL, Sigma-Aldrich) in presence of Brefeldin A (BFA) (10 µg/mL, Sigma-Aldrich), for 4 h at 37 °C 5% CO_2. Cells were washed with ice-cold DPBS (without Ca^{2+} and Mg^{2+}) and incubated with a fixable viability dye (FVD, eFluor506, eBioscience™) at 1:1000, for 30 min on ice. Cells were washed one time

using 150 µL of FACS buffer or Sorting buffer and incubated with 20 µL of FACS/sorting buffer containing anti-mouse CD16/32 FcBlock, for 10 min on ice, Cells were then surface stained with specific prediluted antibodies, for 20 min, on ice.

At this point surface-stained cells were washed twice with ice-cold DPBS, fixed with 1% formaldehyde (Biotium) in DPBS, for 15 min, at RT, in the dark. Cells were then washed twice and resuspended in FACS buffer. Regarding the blood, 25 µL of blood was directly stained and lysed using 1-step Fix/Lyse solution (Thermofisher). Counting beads (AccuCheck counting beads, Molecular Probes, ThermoFisher Scientific) were used to quantify the $CD45^+$ blood cells, following manufacture instructions.

For cell sorting the surface-stained cells were immediately resuspended in 150 µL of Sorting buffer.

For intracellular staining the Foxp3/Transcription Factor Staining Buffer Set (eBioscience™) was used. Upon surface staining, cells were incubated in 100 µL of Foxp3 Fixation/Permeabilization working solution supplemented with BFA, for 30 min, at 4°C. Then, cells were washed with 100 µL 1X Permeabilization Buffer and incubated in Permeabilization Buffer with rat IgG (Sigma-Aldrich) 1:100 and FcBlock 1:500 for 10 min, at 4°C. Intracellular staining mix, containing the appropriate antibodies was added and the cells were incubated for for 1 h, at RT. Cells were washed first in Permeabilization buffer and then in FACS buffer and resuspended in FACS buffer.

Antibodies used for stating were: anti-CD45-FITC (Biolegend), anti-CD45-PerCP-Cy5.5 (Biolegend), anti-Siglec-F-PE (BD Pharmingen), anti-Ly6C-PerCP-Cy5.5 (Biolegend), anti-CD11b-Pe-Cy7 (Biolegend), anti-γδ-APC (Biolegend), anti-γδ-Pe-Cy7 (Biolegend), anti-Ly6G-Pacific blue (Biolegend), anti-Ly6G- APC (Biolegend), anti-Ly6G-FITC (Biolegend), anti-CD5-PE (Biolegend), anti-CD3-Pe-Cy7 (Biolegend), anti-CD3-APC-Cy7 (Biolegend), anti-CD19-APC-Cy7 (Biolegend), anti-CD8- PerCP-Cy5.5 (Biolegend), anti- CD4- Pacific Blue (Biolegend), anti-F4/80-APC-Cy7 (Biolegend), anti-CD69-Pe (Biolegend), anti-CD44- PerCP-Cy5.5 (Biolegend), anti-CD62l-APC (Biolegend), anti- IFN-γ-PE (Biolegend), anti- IL-17-APC(Biolegend).

All incubations were made with protection from light. FVD dilution was in PBS. FcBlock anti-mouse CD16/32 dilution was in FACS buffer or sorting buffer. Foxp3 Fixation/Permeabilization working solution is Fixation/Permeabilization concentrate with Fixation/Permeabilization in 1:3. Permeabilization Buffer dilution was in distilled water.

Flow cytometry acquisition was conducted in BD FACSCanto II, and data was collected using BD Diva software. Post-acquisition analysis was performed using

FlowJo. Single staining using beads were used to calculated compensation on FlowJo. Unstained and single staining performed with cells were used to defined voltages. Gates for each fluorescent marker were defined using fluorescence minus one (FMO) versus samples stained with all markers.

Cell sorting was conducted in FACS Aria II and cells were collected in RPMI complete media with 5% FBS.

2.13. Bacterial killing assays

For bacterial killing assays, mouse neutrophils were FACS sorted from the lungs of P5 pups, based on the expression of SiglecF (sialic acid–binding immunoglobulin-like lectin F) ($CD45^+$ $Ly6G^+$ $CD11b^+$ $SiglecF^{high}$ and $CD45^+$ $Ly6G^+$ $CD11b^+$ $SiglecF^{neg/low}$). Experiments were performed as previously described (112, 113). Briefly, neutrophils were placed in coculture with GBS BM110 with a multiplicity of infection (MOI) of 5, in 200 µL of RPMI complete medium (without antibiotics). The culture plate was centrifuged at 300 g for 5 min, followed by incubation for 1 h at 37 ºC and 5% CO_2. Upon incubation the plate was centrifuged at 1200 rpm for 2 min, the cells were washed two times with PBS, before they were incubated with 200 µg/mL gentamicin for 30 min, at 37 ºC and 5% CO_2. The cells were washed twice in PBS and lysed by resuspension in 100 µL of ice-cold ddH_2O. The number of intracellular bacteria was determined by dilution and plating in TH agar medium o.n. at 37 ºC.

GBS BM110 alone was place in culture as control for bacterial growth, at the end of the 1 h incubation, bacteria were diluted, plated in TH agar medium o.n. at 37ºC and CFU was counted.

2.14. Statistical analysis

All data were analysed with the GraphPad Prism software (v.8.4.2, GraphPad software Inc. CA). Means and standard means (SEM) were calculated, corresponding to the indicated independent experiments. The log-rank (Mantel–Cox) test was used to analyse the survival curve. The Student's t-test was used when analysing two different groups and One-way Anova when more than two groups were included. CFU were log10 transformed. Differences were considered significant for $P \leq 0.05$ and represented by *P < 0.05; **P < 0.01; ***P < 0.001; ****P < 0.0001. The number of samples is express in each legend.

This work is part of the study presented as:

Poster on the XLVII Annual Meeting of the Portuguese Society for Immunology, at Lisboa (20 to 22 April, 2022) - Study of the lung immune response to Group B *Streptococcus* neonatal infection (**Ana Sofia Teixeira** *et al.*)

Results and discussion

Although the immune system is known to play a prominent role in protection against bacterial pneumonia in adults, the mechanisms leading to protective/detrimental immunity and pathology in the neonatal lungs upon bacterial infection remain to be elucidated.

Studies of neonatal pneumonia in the human clinical setting are severely limited. Several experimental models have been exploited to model GBS pneumonia based on aerosolization, intraperitoneal, intranasal, choriodecidual, and via intratracheal inoculation routes (19, 33, 101, 114). These models could generate misleading results, as they use non-natural infection routes, bypassing the mother-to-newborn transmission of GBS and the normal course of the disease in humans. Our group recently developed a clinically relevant neonatal mouse model of GBS infection that mimics the natural infection in human newborns, which leads to pneumonia (22). Thus, in this work, I investigated the infection progression and disease severity, as well as the immune response in the neonatal lung, aiming to gain insight into the mechanistic basis of GBS early-onset disease.

3.1. Characterization of a neonatal mouse model of GBS pneumonia

Our established model was developed in the BALB/c mice (22). Owing to the utility and applications of models in C57BL/6 mice, such as the availability of several transgenic mouse lines in this background, we started by adapting our previously described model for this strain. To this end, pregnant C57BL/6 female mice are i.vag. inoculated with the GBS hypervirulent strain BM110 at gestational days 16 and 17 and allowed to deliver spontaneously, as schematized in Figure 2A. Infection in the offspring was monitored for 5 days. During this experimental period, we evaluated the survival and general welfare of infected mice as compared to pups born from uninfected control mothers. At specific time points, we investigated more specific parameters, namely the weight gain, bacterial burden, and histopathology in the lung.

The survival curve analysis revealed that approximately 58% of pups born from colonised progenitors succumbed to disease during the first three days of life, with the highest percentage of mortality (~30%) occurring between P0 and P1 (Figure 2B), possible due to fulminant septicaemia. During the first three days of life, infected pups had to be humanely euthanised when they began to display severe symptoms, including poor suckling (no milk spot), purple skin, dehydration, and painful abdominal palpation, parameters previously defined for the poor neonatal outcome (115). No more deaths

were registered after day 3. These results contrast significantly with the percentage of mortality of 0% observed in the control group, the uninfected animals (Figure 2B). Interestingly, however, despite close monitoring of infected pups, commonly animals did not present severe symptoms and died. A possible explanation for this observation is GBS dissemination leading to quick progression from pneumonia to septicaemia and/or meningitis and, consequently, entailing animal death.

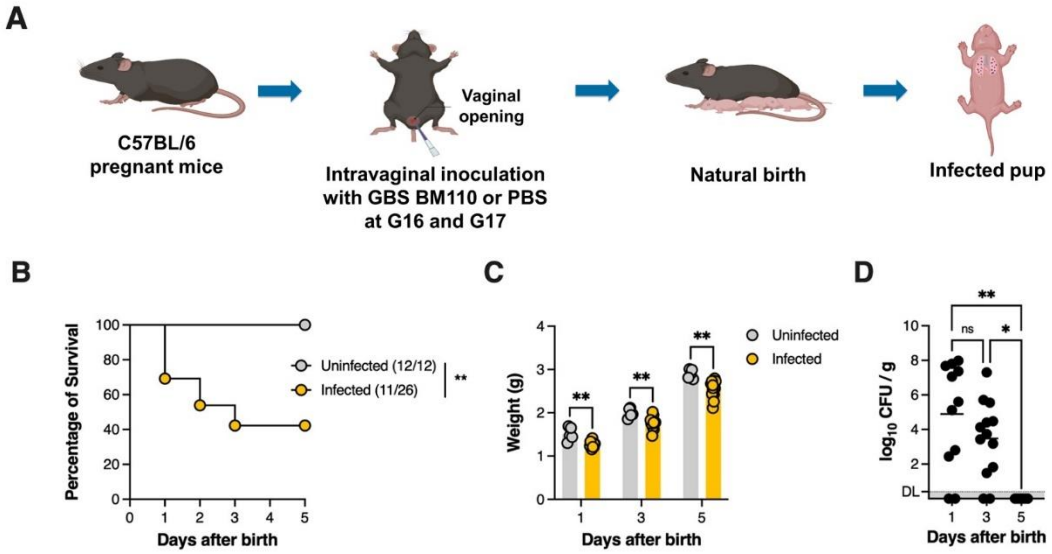

Figure 2. **GBS vertical transmission leads to lethal neonatal pneumonia. (A)** A schematic illustration of the colonisation model is shown. Pregnant C57BL/6 female mice were intravaginally colonised with $8x10^4$ CFU GBS hyper virulent strain BM110 or PBS, at gestational days 16 and 17. Figure created in Biorender. **(B)** Kaplan-Meier survival curve of neonatal mice born from GBS-colonised dams, monitored during a 5 days' period. The numbers in parentheses represent the number of animals that survived versus the total number of animals born. **(C)** Newborns were weighted at postnatal days 1, 3, and 5. Data are presented as mean ± SEM [n=5 (Uninfected); n=12 (Infected)]. **(D)** Newborn mice were sacrificed at postnatal days 1, 3, and 5 and the lung bacterial loads were determined. Data are presented as mean [n=11 (P1); n=12 (P3); n=6 (P5)]. Each symbol indicates data from single pup. Comparisons by one-way ANOVA. Statistical differences (P values) between groups are indicated. * $P < 0.05$; ** $P < 0.01$; *** $P < 0.001$; ns – not significant; DL – Detection Limit.

Furthermore, when comparing the body weight of infected animals with aged-matched uninfected animals, we verified a significant decrease in all the time points studied (Figure 2C).

We next evaluated the progression of infection by enumerating the bacterial colonisation in the neonatal lung at different time points upon delivery. The lung is the first organ to be in contact with the bacteria during birth due to aspiration of maternal vaginal secretions during delivery (1, 24, 33). Therefore, it is also where the first colonisation occurs and where the immune response to the pathogen initiates. The evaluation of bacterial colonisation in the lungs, through serial dilutions, showed the maximum burden of bacterial colonisation at P1 with a slight but not significant reduction at P3. At P5, infection appears to be resolved in the lungs as no bacteria were detected at this time point (Figure 2D), even though pups still presented decreased body weight.

This indicates that the infection not only leads to mortality but, as sequel, also leads to decrease weight gain in the surviving animals, even when the infection appears to be resolved in P5. Nevertheless, we cannot exclude an active infection as pups could still be colonised in other organs, such as the liver and the brain, at this time point. Alternatively, the decreased weight could be a consequence of infection, and reduced suckling. With age, surviving pups exposed to neonatal infection recovered their weigh to levels similar to age-matched uninfected controls (data not shown).

GBS EOD is heralded by respiratory complications, including hypoxia and pulmonary hypertension, that lead to pneumonia (2, 9, 39). Pneumonia is a condition known to cause histologic alterations in the lung (116). Thus, a relevant way to assess pulmonary disease severity is the evaluation of the histopathology of infected lungs. Some of the alterations caused by neonatal GBS pneumonia have already been described in the 1970s (117). Histologic evidence of lobar or multilobar pneumonia has been found in 80% of babies that died from EOD (117). However, the analysis was superficial and obtained from severe fatal cases, and thus more detailed information regarding lung pathology is needed. Therefore, to characterise in more depth the alterations caused by GBS pneumonia, H&E staining was made to evaluate histological alterations. Moreover, Giemsa staining was also performed to evaluate the infiltration of neutrophils as well as the presence of alveolar macrophages. Histopathology analyses were made in lung sections from time points with detectable bacterial burden, the P1 and P3. When observing the lung sections, four anatomic structures were defined, namely the interstitium, airways, alveoli, and blood vessels. The findings we mainly observed and used in the histological scores were haemorrhage, congestion, septal thickening, atelectasis, neutrophil infiltration, and presence of alveolar macrophages (Figure 3A). Representative images of the temporal development of pathology are shown in Figure 3A.

When comparing the total histological scores, we found that the extent of lung histopathological alterations in the lung of P1 infected animals do not differ from the respective age-matched uninfected controls (Uninfected, 7.33 ± 0.88; Infected, 9.00 ± 1.817). Interestingly, uninfected pups did not present a histopathology score of 0, suggesting that the observed alterations are not a result of infection but rather from the adaptations of the tissue to the external environment that can still be occurring at P1 (Figure 3B). Nevertheless, the experimental sample size of uninfected controls is reduced at this time point ($n = 3$) and needs to be increased to fully validate this observation.

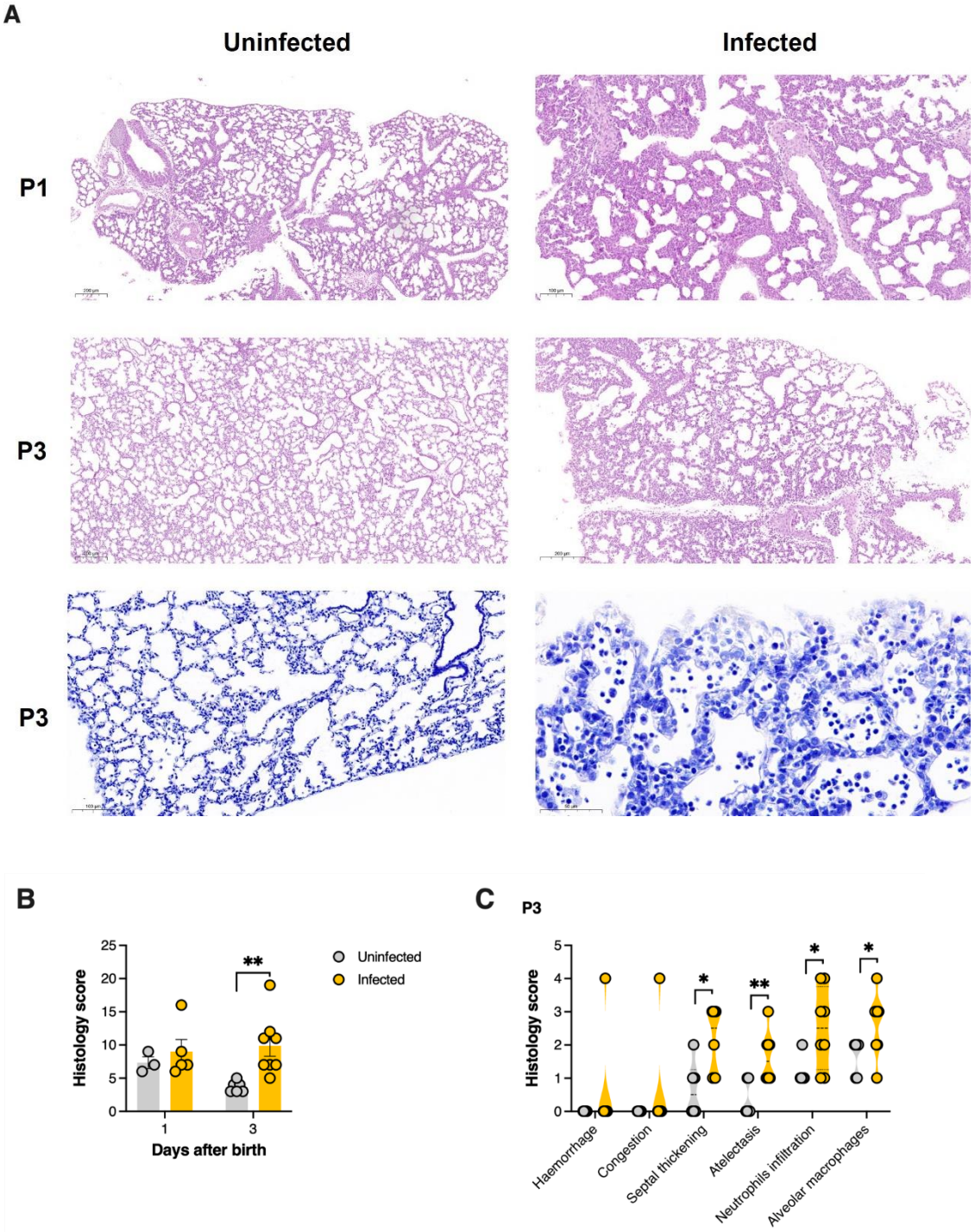

Figure 3. Histopathology of the neonatal lung upon GBS pneumonia. Pregnant C57BL/6 female mice were intravaginally colonised with $8x10^4$ CFU GBS hyper virulent strain BM110 (Infected) or PBS (Uninfected), at gestational days 16 and 17. Analyses were performed at the indicated time points. **(A)** Representative images of lung stained with H&E are showed for each time point**.** Giemsa staining was made at P3. Scale bars 200µm (H&E: Uninfected, P1 and P3; Infected, P3); 100 µm (Giemsa: Uninfected, P3. H&E: Infected, P1); 50 µm (Giemsa: Infected P3) **(B)** Global histological score. Histopathological alterations were evaluated and classified in separated histological scores and added to give a global histological score. Data are presented as mean ± SEM [n=3 (P1, Uninfected); n=5 (P1, Infected); n=6 (P3, Uninfected); n=8 (P3; Infected)] **(C)** Summary of histological analysis from the lung of GBS-infected pups at P3. Data are presented as violin plot showing all points. [n=6 (Uninfected); n=8 (Infected)]. Each symbol indicates data from single pup. Comparisons by Student's *t*-test. Statistical differences (P values) between groups are indicated. * $P < 0.05$; ** $P < 0.01$.

At P3, infected animals presented a significant increase in the total histological score compared to age-matched controls (Figure 3B). When analysing individually each of these findings, we found that infected animals were characterized by increased septal thickening, atelectasis, higher neutrophil infiltration, and the presence of alveolar macrophages (Figure 3C). At this time point, the infection appears to be the factor leading to a worse condition of the neonatal lung, reflected in a higher histological score. This result is consistent with a previous observation in a primate model of neonatal GBS disease, where a high bacterial burden was found in the lungs, with the presence of interalveolar and interstitial monocytic infiltrates, polymorphonuclear cells in the alveoli, atelectasis, and loss of alveolar architecture (118).

Collectively, these data indicate that GBS vertical transmission leads to lung colonisation and pulmonary lesions consistent with pneumonia.

3.2. Immune cellular dynamics during GBS neonatal pneumonia

The neonatal immune response during neonatal GBS infection is thought to be strongly associated with the progression of infection and disease outcome (104, 119). However, the host immune response in the site of infection during, and after the onset of disease, has been poorly characterized. Therefore, we next continued the lung analysis by mapping of the dynamic of immune response to infection over the pups' first five days of life and compared it to age-matched uninfected animals.

Both myeloid and lymphoid populations were evaluated by multiparametric flow cytometry at P1, P3 and P5. The gating strategy used to define the populations of myeloid and lymphoid cells is shown in Figure 4A and Figure 4B, respectively.

Within the myeloid cells three cell populations were studied, the eosinophils, the inflammatory monocytes, and the neutrophils. We found a significant decrease in the frequency of eosinophils at P1 and P3 in the lungs of infected pups when compared to uninfected controls (Figure 4C). However, their total number did not differ between groups (Figure 4C). By P5 although its relative percentage was similar between groups, the numbers were significantly increased in infected animals (Figure 4C). The inflammatory monocytes have a different profile in infected animals as their frequency was a significantly higher at P1. Regarding cell numbers, infected animals presented increased values when compared to uninfected controls, reaching significance at P3 and P5 (Figure 4C). Analyses of neutrophils showed a tendency towards higher numbers at P1 and a significant increase in both the frequency and numbers in infected animals at P3 compared to the uninfected control neonates. This increase in numbers was still

observed at P5 (Figure 4C). This recruitment of neutrophils into the infected organ is consistent with a protective immune response, aiming to eliminate bacteria.

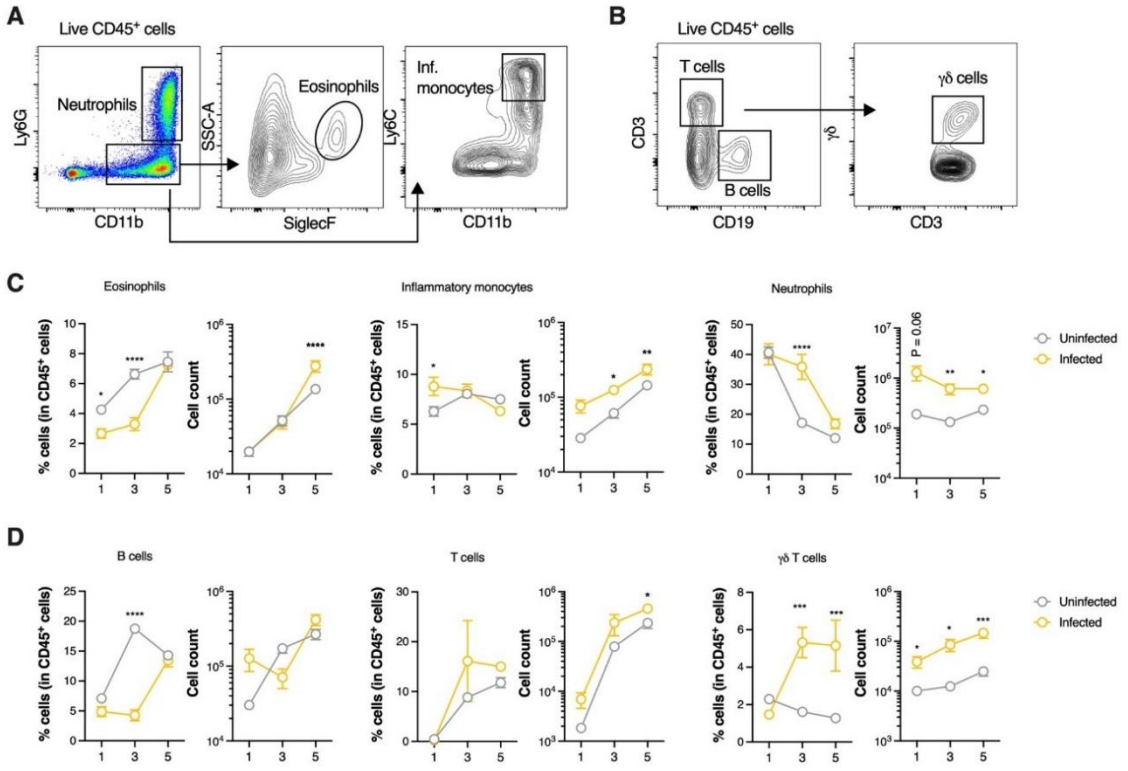

Figure 4. Evaluation of myeloid and lymphoid populations during GBS pneumonia by multiparametric flow cytometry. Pregnant C57BL/6 female mice were intravaginally colonised with $8x10^4$ CFU GBS hyper virulent strain BM110 (Infected) or PBS (Uninfected), at gestational days 16 and 17. Animals from uninfected and infected groups were sacrificed at indicated time points and the lung was collected for flow cytometry analysis of myeloid and lymphoid cell population. **(A)** Representative gating strategy used to define the myeloid cells. Cells where gated in live $CD45^+$ cells. Neutrophils were defined as $CD11b^+Ly6G^+$, eosinophils were defined as $CD11b^+Ly6G^-SiglecF^+SSC\text{-}A^{int/high}$, inflammatory monocytes were defined as $CD11b^+Ly6G^-Ly6C^{high}$. **(B)** Representative gating strategy used to define lymphoid cells. Cells where gated in live $CD45^+$ cells. T cells were defined as $CD3^+CD19^-$, B cells were defined as $CD3^-CD19^+$, γδ T cells were defined as $CD3^+CD19^-$ $γδ^+$. **(C)** Frequency and number of indicated myeloid cells. Data is presented as mean ± SEM, each symbol represents data from single pup [n= 6 (P1, uninfected); n=11 (P1, infected); n=11 (P3, uninfected); n=10 (P3, infected); n= 7-8 (P5, uninfected); n=8 (P5, infected)]. **(D)** Frequency and number of indicated lymphoid cells. Data is presented as mean ± SEM, each symbol represents data from single pup [n= 6 (P1, uninfected); n=11 (P1, infected); n=5-8 (P3, uninfected); n=10 (P3, infected); n= 7-8 (P5, uninfected); n=8 (P5, infected). Statistical differences (P values) between groups are indicated. * $P < 0.05$; ** $P < 0.01$; *** $P < 0.001$; **** $P<0.0001$

Regarding the lymphoid cells, we studied the B cells, the T cells and the γδ T cells. Between these three cells populations, the one that is markedly altered in the infected neonates is the specific subset of T cells, the γδ T cells, as it has a significant increase in numbers at P1 and a significant increase both in frequency and numbers at P3 and P5, suggesting that they could be recruited or expanding in response to infection (Figure 4D). As for the total $CD3^+$ T cells, this population only showed a significant difference in cell counts at P5, with a higher number of cells in infected pups when compared with controls (Figure 4D). The frequency of B cells quickly increased from P1 to P3 in control pups. This was not observed in infected animals, which presented a

significant decreased percentage at P3. By P5, no differences were observed in the frequency of B cells between groups (Figure 4D).

Overall, the frequencies found in the uninfected control pups are in accordance with a previous report showing that granulocytes peak in the lung at P1, decreasing thereafter, while eosinophils increase (120). Similarly, to their results, T and B cells were very low after birth and gradually increased over time (120). We and others have previously shown that during neonatal GBS infection, bacterial clearance is commonly attributed to neutrophils, the most abundant circulating leukocyte (97, 104, 121, 122). Here, we found that infected pups were able to efficiently recruit these effector cells into the lung early upon infection.

Neutrophil recruitment to infected tissues, hallmarks of inflammation and bacterial infections, is in part driven by IL-17A. IL-17 triggers stromal cells in the bone marrow to produce granulocyte colony-stimulating factor (G-CSF), which promotes neutrophil development and release into the circulation (123). Indeed, IL-17A plays an essential role in lung immunity to bacterial infections (124-128) . Thus, we sought to determine whether this cytokine was increased during neonatal pneumonia and its cellular source. γδ T cells are a population of innate-like lymphocytes and an important source of IL-17A, and we have found that these cells were increased during neonatal GBS pneumonia. γδ T cells are the first T cells to appear in the thymus during development, presenting characteristics from both adaptative and innate immunity responses, as they can be rapidly mobilized and expanded upon infection in response to cytokines, PAMPs and DAMPs, and recognize a wide range of antigens, even during infancy, while also expressing the hallmark of adaptive immunity, the T cell receptor (TCR) (79-81). After their egress from the thymus, γδ T cell subsets establish residency in predetermined locations, preferentially at barrier sites, such as the lung (80, 88). In mice, γδ T cells are mainly characterized by their development to produce, except in rare occasions, IFN-γ or IL-17A (129, 130).

We pursued a more thorough study of the γδ T cells profile, with the evaluation through flow cytometry of the production of IFN-γ or IL-17A. The time point studied was P3, as it was shown to be a time point where the immune response is actively taking place, with animals presenting higher pulmonary pathology while also coinciding with the start of the alveolar phase of lung development (120). The gating strategy used to define the γδ T cells population and IFN-γ- or IL-17A-producing γδ T cells is shown in Figure 5A.

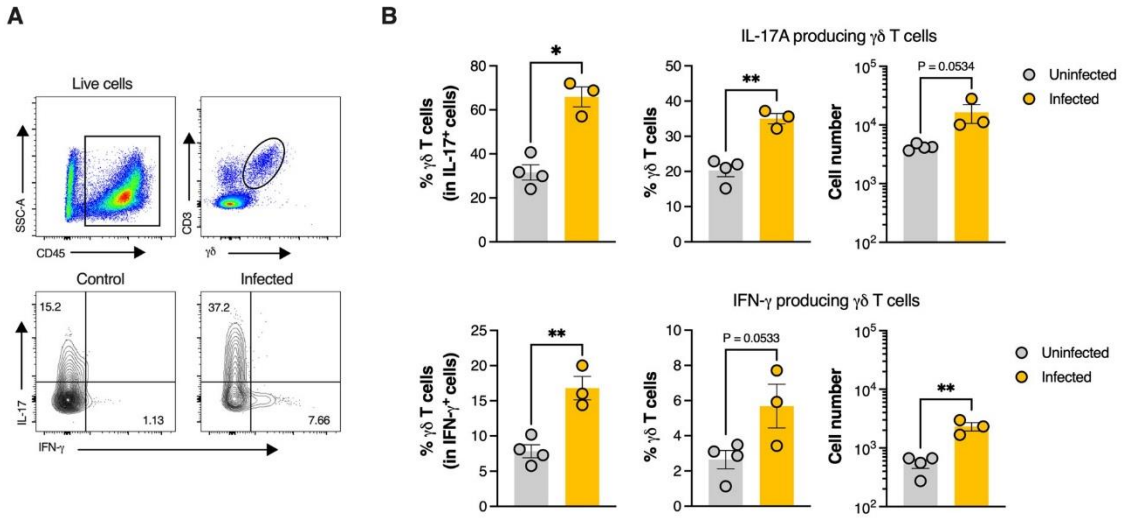

Figure 5. γδ T cells profile during GBS pneumonia. Pregnant C57BL/6 female mice were intravaginally colonised with 8x10^4 CFU GBS hyper virulent strain BM110 (Infected) or PBS (Uninfected), at gestational days 16 and 17. Animals from uninfected and infected groups were sacrificed at P3 and the lung was collected for flow cytometry analysis of γδ T cells. **(A)** Representative gating strategy used to define γδ T cells and IL-17A and IFN-γ positive cells. Live cells were gated in SSC-A vs CD45$^+$ cells. The following cells were gated within CD45$^+$ cells. γδ T cells were defined as CD3$^+$ γδ$^+$. The intracellular markers IL-17A or IFN-γ were analysed withing γδ T. **(B)** Frequency and number of γδ T cells in the respective gate. Data is presented as mean ± SEM, each symbol indicates data from a single pup [n= 4 (uninfected); n= 3 (infected)]. Comparisons by Student's *t*-test. Statistical differences (P values) between groups are indicated. * P < 0.05; ** P < 0.01.

Our results show that γδ T cells were predominantly IL-17A-producers in the lung of neonatal mice, although IFN-γ-producers could also be detected. Although in both cases, infection led to increase frequency of IL-17A- and IFN-γ-producing γδ T cells, this increase was more pronounced in the IL-17A subset (Figure 5A and 5B). Upon gating on IL-17-positive cells, we found that the lungs of pups infected with GBS presented high frequencies of γδ T cells among total IL-17-producing cells, accounting for approximately 70% of total IL-17-producing cells in this tissue (Figure 5B).

Collectively, these data show that neonatal γδ T cells quickly respond to infection and are a primary source of IL-17A in response to bacterial challenge. Moreover, our results suggest that this mechanism might have an important role in bacterial clearance, where γδ T cells produce IL-17A leading to the recruitment of neutrophils into the lungs and likely inducing the production of antimicrobial peptides (80, 87, 130).

Interestingly, γδ T cells have also been associated with lung homeostasis, tissue repair and maintenance of barrier integrity (e.g., by promoting epithelial cell survival) (80, 131). Therefore, to investigate whether γδ T cells could remain altered due to the infection at later time points, we studied animals at P15. We chose to analyse this time point as it entails the peak of the pulmonary immune system development in the alveolarisation period and the beginning of microvascular maturation (120).

Firstly, it is important to note that for this part of my dissertation, we used the spleen as a term of comparison for the lung, considering that this organ reflects the state of the systemic immune system of the mice (132).

No differences were observed in the number of γδ T cells between infected and uninfected animals in both organs (Figure 6A). Evaluation of the number of myeloid cells (eosinophils, inflammatory monocytes, and neutrophils) also revealed no differences between groups (Figure 6B).

Immunological memory is a hallmark of the adaptive immune system. γδ T cells have the hallmark ability of resident memory αβ T cells and adaptive-like responses to undergo rapid stimulation and expansion upon a secondary infection (79, 133, 134). Therefore, we also analysed the residency profile of γδ T cells using the gating strategy presented in Figure 6C. This gating strategy allowed us to determine the expression of the residency markers CD69, CD44 and CD62L. The residency profile is known to have an upregulation of CD69 (135, 136) and CD44 (137-139), whereas CD62L is downregulated (140, 141). This analysis revealed that γδ T cells present in the lung of P15 infected animals might have the same number, but their profiles are different from the cells in uninfected controls, as animals that survived neonatal pneumonia showed a significantly higher percentage of cells with the $CD69^{+}CD44^{+}CD62L^{-}$ tissue residency profile (Figure 6D). This phenotype was not observed in the spleen (Figure 6D). Overall, these results suggest that although γδ T cells numbers were similar to controls after bacterial clearance, they reside in the lungs following neonatal pneumonia as tissue-resident cells and might have the capacity to rapidly expand following secondary challenge.

To complete this section of our study a histological evaluation of lung was made, and a histological score was attributed. The infected animals presented a larger area of tissue with histopathological alterations, with at least three findings present at the same time. This is reflected in a significantly higher histological score for the infected animals, meaning that these animals might have respiratory sequels due to neonatal infection (Figure 6F). Early life exposures to environmental challenges are known to be associated with airway immune disorders (142). The hypothesis that survivors to neonatal GBS pneumonia could have subsequent changes on adult lung homeostasis and host defence was not explored.

We hypothesized that IL-17A-producing γδ T cells provide a first line of defence against GBS pneumonia. To determine the contribution of γδ T cells to host protection against GBS disease, survival and bacterial colonisation studies were made in

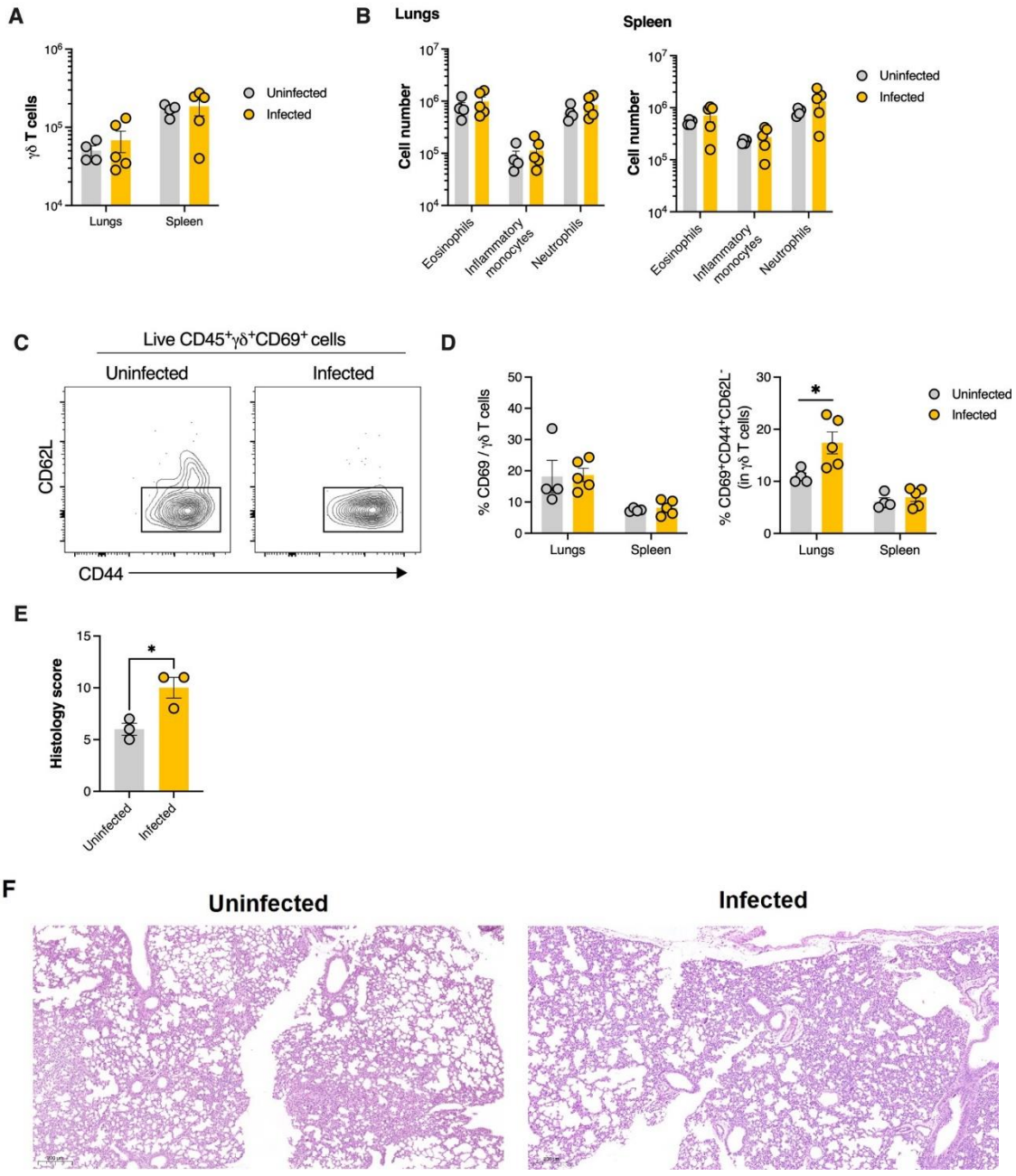

Figure 6. Immunological cell profile and histological analysis after recovery from neonatal pneumonia. Pregnant C57BL/6 female mice were intravaginally colonised with $8x10^4$ CFU GBS hyper virulent strain BM110 (Infected) or PBS (Uninfected), at gestational days 16 and 17. Animals from uninfected and infected groups were sacrificed at P15. The lung and the spleen were collected for flow cytometry analysis of γδ T cells and myeloid cells. The lung was also collected for histological analysis. **(A)** Frequency and number of γδ T cells. Data is presented as mean ± SEM [n= 4 (uninfected); n= 5 (infected)]. **(B)** Frequency and number of indicated myeloid cells. Data is presented as mean ± SEM [n= 4 (uninfected); n= 5 (infected)]. **(C)** Representative contour plots of tissue resident γδ T cell. The profile of tissue resident of γδ T cells was define by $CD45^+γδ^+CD96^+CD44^+CD62L^-$. **(D)** Frequency of indicated cell populations among γδ T cells. Data is presented as mean ± SEM [n= 4 (uninfected); n= 5 (infected)]. **(E)** H&E staining was made in P15 animals, and a global histological score was calculated by adding separated histological scores de specific findings. Data are presented as mean ± SEM [n=3 (uninfected); n= 3(infected)]. **(F)** Histological representation of lung in H&E staining. Scale bars 200µm. Each symbol indicates data from single pup. Comparisons by Student's *t*-test. Statistical differences (P values) between groups are indicated. * $P < 0.05$

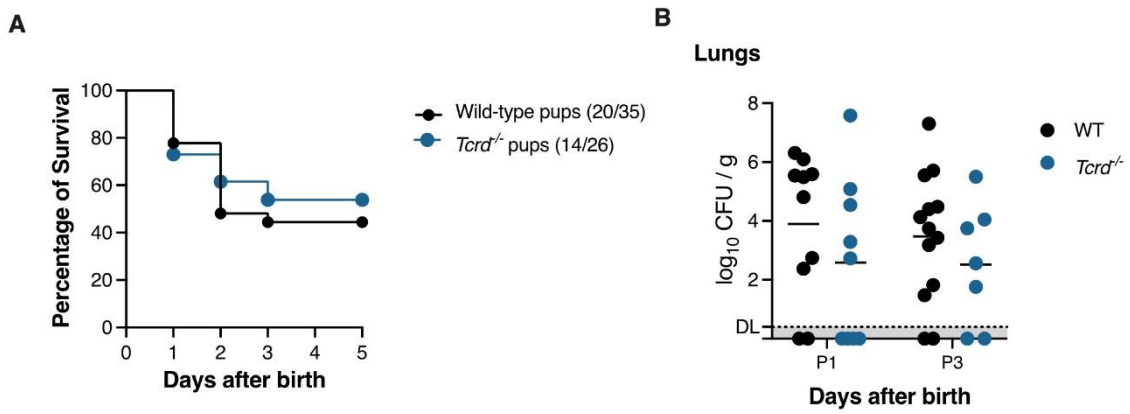

Figure 7.Assessment of γδ T cells role as first line of defence against neonatal bacterial pneumonia. Pregnant C57BL/6 (wild-type) or γδ T cell receptor-deficient (Tcrd$^{-/-}$) female mice were intravaginally colonised with 8x10^4 CFU GBS hyper virulent strain BM110, at gestational days 16 and 17. **(A)** Kaplan-Meier survival curve of wild-type and Tcrd$^{-/-}$ neonatal mice born, monitored during a 5 days' period. The numbers in parentheses represent the number of animals that survived versus the total number of animals born. **(B)** Newborn mice were sacrificed at postnatal days 1 and 3 and the lung bacterial loads were determined. Data are presented as mean [n=10 (P1, WT); n=9 (P1, Tcrd$^{-/-}$); n=13 (P3, WT); n=7 (P3, Tcrd$^{-/-}$)]. Each symbol indicates data from a single pup.

homozygotic TCRδ$^{-/-}$ mice. Surprisingly, no differences were found in the survival between TCRδ$^{-/-}$ pups compared with isogenic C57BL/6 control mice (Figure 7A). Moreover, the bacterial colonisation in the lung of TCRδ$^{-/-}$ pups did not differ from the WT, at P1 and P3 (Figure 7B).

Our results suggest that, contrary to what we initially believed, γδ T cells do not have a protective role in the acute phase of GBS infection. However, we cannot exclude their impact on bacteria clearance as, unfortunately, until the date of delivery of this dissertation, it was not possible to include later time points. It would be interesting to address whether TCRδ$^{-/-}$ mice are efficiently able to eliminate GBS from the lung at later time points. It is possible that the recruitment of neutrophils is not impaired in TCRδ$^{-/-}$ pups, as there are other contributing factors, including chemokines and the adhesion cascade involved in neutrophil extravasation. Moreover, it has been proposed that γδ T cells participate in the resolution of inflammation following bacterial clearance, in a mouse model of acute *Streptococcus pneumoniae* lung inflammation, by promoting cytotoxicity against mononuclear phagocytes to decrease numbers to homeostatic levels (143). Thus, pulmonary histopathology, immune cells profiling and inflammatory mediators, such as pro-inflammatory cytokines, should also be evaluated in these animals.

3.3. GBS neonatal pneumonia leads to accumulation of SiglecF expressing neutrophils

To understand what could be leading to animals' death, we stratified our analysis by disease severity. The time point studied was P3, as we have found that it is a time

point with detectable bacterial burden and where an active immune response is occurring. Furthermore, P3 is a time point where the signs of physical distress in severe animals are clearly manifested, and we can determine precisely which animals will live or die.

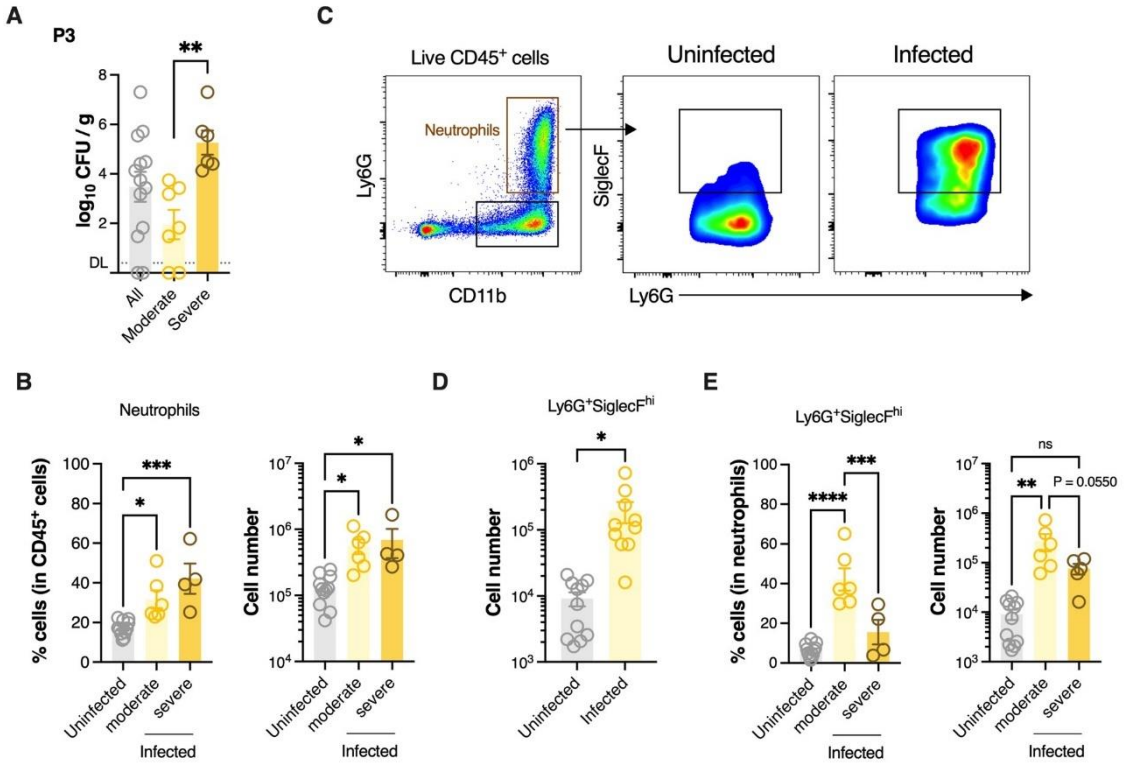

Figure 8. Evaluation of lung colonisation and neutrophil population according to disease severity. Stratification was made by dividing data All (all infected animals), Moderate (infected animals with moderate signs of disease) and Severe (infected animals with severe signs of disease). **(A)** Newborn mice were sacrificed at postnatal days 3 and the lung bacterial loads were determined by disease severity. Data are presented as mean [n=13 (all); n=7 (moderate); n=6 (severe)]. **(B)** Frequency and number of neutrophils in uninfected, moderate and severe groups. Data is presented as mean ± SEM [n= 11 (uninfected); n= 6 (moderate); n= 4 (severe)]. **(C)** Representative gating strategy used to define neutrophils profile. Cells were gated in live CD45$^+$ cells. Neutrophils were defined CD11b$^+$Ly6G$^+$. Profile of neutrophils was defined as CD11b$^+$Ly6G$^+$SiglecF^{hi} or CD11b$^+$Ly6G$^+$SiglecF$^{neg/low}$. **(D)** Number of SiglecF^{hi} neutrophils in uninfected and infected animals. Data are presented as mean ± SEM [n=11 (uninfected); n=10 (infected)]. **(E)** Frequency and number of SiglecF^{hi} neutrophils in the lung of infected pups according to disease severity. Data are presented as mean ± SEM [n=11 (uninfected); n=6 (moderate); n=4-5 (severe)]. Each symbol indicates data from single pup. Comparisons by one-way ANOVA. Statistical differences (P values) between groups are indicated. * P < 0.05; ** P < 0.01; *** P < 0.001; **** P < 0.0001; ns - not significant.

We immediately observed in this stratified evaluation that severe animals did not have the same capacity to control infection as those with moderate disease, as they presented significantly higher bacterial colonisation in the lung (Figure 8A). Based on previous results (Figure 4C) showing that infected pups can recruit neutrophils to the lung in early time points of infection, we appraised if this population was altered in severe animals. The obtained results showed that both pups with moderate or severe disease had significantly higher frequency and numbers of neutrophils than the uninfected controls (Figure 8B). Surprisingly, no differences were observed in this population between pups with moderate or severe GBS disease (Figure 8B). When we analysed deeper the lung neutrophils phenotype during neonatal pneumonia, we unexpectedly

found a neutrophil population that coexpressed the eosinophil-specific surface marker SiglecF (Figure 8C). The SiglecF^{hi} subset was found higher in numbers in infected animals (Figure 8D). This population was rare in uninfected animals. Furthermore, the pups with moderate signs of disease presented a significant increase in the frequency of SiglecF^{hi} neutrophils within the neutrophil population. This increase was not observed in the severe animals, suggesting that this population could be important for bacterial clearance and survival (Figure 8E).

To study whether SiglecF^{hi} neutrophils have increased capacity to clear bacteria, we sorted neutrophils from the neonatal lung, based on their expression of SiglecF ($CD45^+$ $Ly6G^+$ $CD11b^+$ SiglecF^{hi} and $CD45^+$ $Ly6G^+$ $CD11b^+$ SiglecF$^{neg/low}$), and performed a bacterial killing assay. Neutrophils from both subsets were incubated with GBS (MOI=5), and the percentage of phagocytosis was obtained. The results revealed a significant increase in the percentage of phagocytosis by the SiglecF^{hi} subset (Figure 9). This result sustains our hypothesis that this population can be important for bacterial clearance in the lung during neonatal GBS pneumonia.

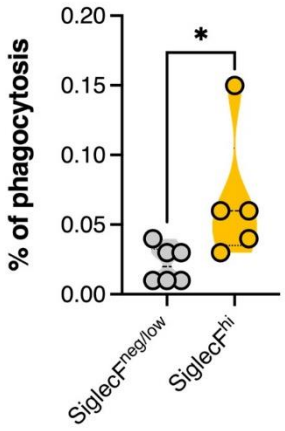

Figure 9. SiglecF^{hi} ability to clear GBS. SiglecF^{hi} and SiglecF$^{neg/low}$ were sorted from the neonatal mouse lung and infected with $3x10^4$ cells of GBS BM110, at a MOI of 5 bacteria per cell, for 1 h. After this time, cells were washed and further incubated with culture media containing gentamycin. CFUs were determined by serial dilution plating. Data are presented in a violin plot and are pooled from two independent experiments [n=6 (SiglecF$^{neg/low}$); n=5 (SiglecF^{hi})]. Each symbol indicates a replica. Statistical differences (P values) between groups are indicated. Comparisons by Student's *t*-test. * $P < 0.05$.

To gain further knowledge on the origin of the SiglecF^{hi} neutrophils in the neonatal lung during GBS pneumonia, we searched for this population in the peripheral blood of infected pups and compared it with uninfected controls at P3. The objective of this analysis was to determine if the circulating neutrophils found in pups with moderate disease already presented this phenotype and therefore contributing to the population observed in the lungs, or if the expression is similar to uninfected animals indicating that SiglecF$^{neg/low}$ neutrophils acquires the profile of SiglecF^{hi} neutrophils by stimuli given by the lung environment.

The results show that the number of total circulating neutrophils as well as the frequency of the SiglecF^{high} subset among neutrophils did not differ between groups (Figure 10A and 10B). Moreover, analysis of the mean fluorescence intensity (MFI)

showed no differences in the levels of SiglecF expression in the cell surface (Figure 10C).

Altogether these results suggest that the neutrophils develop a SiglecF^{hi} profile in the lung where they contribute to bacterial clearance. SiglecF-expressing neutrophils were discovered only very recently and have been implicated in several diseases, including lung tumour, infarcted heart, airway inflammation and allergy, chronic kidney disease, and bacterial infection (125, 144-149). These cells have been shown to have higher ability to produce ROS and form neutrophil NET(125, 145), which could lead to increases capacity to control bacteria in our model. We are now trying to identify the factors that induced conventional neutrophils to convert into SiglecF^{hi}.

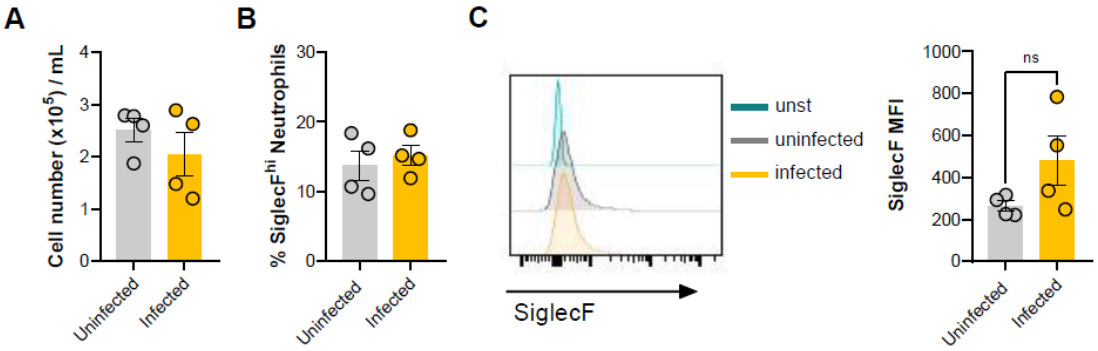

Figure 10. Evaluation of circulating neutrophils in peripheral blood. Pregnant C57BL/6 mice were intra-vaginally inoculated with 8x10^4 CFU of GBS hyper virulent strain BM110 or PBS (uninfected) at gestational days 16 and 17. Analyses were performed in the progeny at P3. **(A)** Cell number of circulating neutrophils per mL of blood. **(B)** Percentage of SiglecF^{hi} neutrophils in circulation. **(C)** Quantification of SiglecF on neutrophils, presented as mean fluorescence intensity (MFI). Representative histograms are shown. Yellow line, infected pups with moderate disease; Grey line, uninfected pups; Green line, unstained. Data are presented as mean ± SEM [n=4 (uninfected); n=4 (infected)]. Each symbol indicates data from single pup. Comparisons by Student's *t*-test. ns – not significant.

3.4. Local inflammatory response during GBS neonatal pneumonia

Finally, we investigated possible differences in cytokine gene expression as a result of disease severity at P3. To this end, the expression of pro- and anti-inflammatory cytokines genes was analysed by RT-qPCR. The relative gene expression level is presented after normalisation to the reference gene *Hprt*.

The expression of the pro-inflammatory cytokine *Il1b* was significantly increased in severe animals as compared to uninfected animals. A tendency towards higher expression was also observed when severe animals were compared to the moderate group (P = 0.0827) (Figure 11A). The expression of *Tnfa, Il33* and *Il17* was not different between groups, although a tendency to increase expression of *Tnfa* in severe animals was observed (Figure 11A). The expression of *Il17* was only observed in pups with moderate disease, but no differences were found among the groups (Figure 11A). The

expression of the anti-inflammatory cytokine *Il10* also showed a tendency for upregulation in severe animals (Figure 11A).

These results contradict our hypothesis as we expected a profile of inflammation more heightened in the infected animals, particularly in the severe group. Nevertheless, the expression of cytokines such as IL-1*β* can be regulated post-transcriptionally, for example by miR-223 (25). Therefore, to clarify whether the observed expression levels are correlated at the protein level, in the future, we will perform protein quantification in the neonatal lung using immunoassays such as ELISA (Enzyme-Linked Immunosorbent Assay).

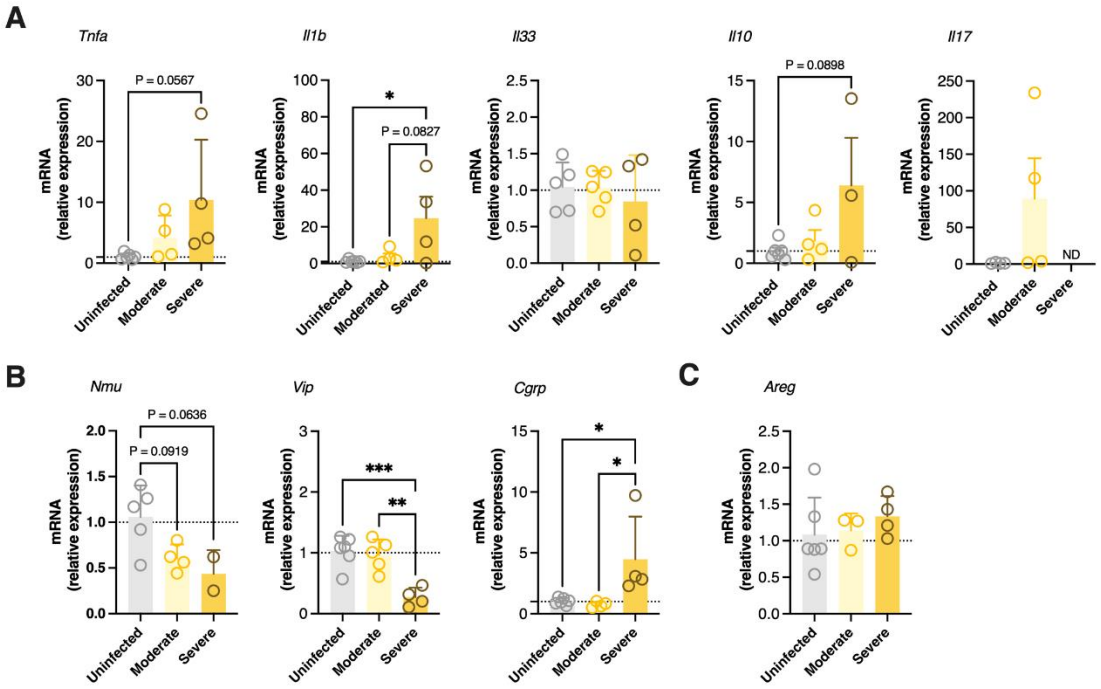

Figure 11. Evaluation of inflammatory state of lung and neuropeptide expression during neonatal pneumonia. Pregnant C57BL/6 mice were intra-vaginally inoculated with 8x10^4 CFU of GBS hyper virulent strain BM110 or PBS (Uninfected) at gestational days 16 and 17. Analyses were performed in the progeny at P3. Relative gene expression evaluated by RT-qPCR, normalized for the reference gene *Hprt*. Samples are stratified by disease severity. **(A)** Relative expression of the pro- and anti-inflammatory cytokines *Tnfa*, *Il1b*, *Il33*, *Il10* and *Il17*. **(B)** Relative expression of the neuropeptides *Nmu*, V*ip* and *Cgrp*. **(C)** Relative expression of *Areg.* Data are presented as mean ± SEM [n=4-6 (uninfected); n=3-5 (moderate); n=2-4 (severe)]. Each symbol indicates data from single pup. Comparisons by one-way ANOVA. Statistical differences (P values) between groups are indicated. * P < 0.05; ** P < 0.01; *** P < 0.001; ND - Not detected.

It is becoming increasingly recognized that the regulation of immunity by the nervous system is essential for proper tissue homeostasis and protection. Only in recent years studies have shown that peripheric neurons, such as sensory neurons, can locally release neuropeptides which in turn can regulate immunity through signalling *via* functional neuropeptides receptors expressed by these cells (150, 151). Pulmonary neurons express several neuropeptides including neuronal-derived vasoactive intestinal peptide (VIP), Substance P, neuromedin U (NMU) and calcitonin gene-related peptide (CGRP), among others (151). Interestingly, multiple studies have shown that these

neuropeptides can regulate immunity against bacteria (reviewed in (151)). Thus, we next evaluated the gene expression levels of *Nmu*, *Vip* and *Cgrp*. Although not significant, we found a tendency for decreased expression of *Nmu* (Figure 11B). NMU, produced by cholinergic neurons, has been implicated in type 2 immunity, amplifies allergic inflammation, and is involved in protective responses against helminthic infections as well as neonatal influenza infection (152, 153). The expression of *Vip* was downregulated in severe animals when compared to both uninfected and animals with moderate disease (Figure 11B). As for the *Cgrp,* the opposite profile of expression was observed as the relative expression of this gene is higher in severe animals compared with both pups with moderate disease and uninfected controls (Figure 11B). VIP is an immunoregulatory neuropeptide that has been described to dampen the production of pro-inflammatory cytokines (154). The release of CGRP has been showed to be a mediator of immune suppression in pulmonary tissue, more in specific by suppressing neutrophil recruitment and γδ T cell-mediated defence during bacterial lung infections (113). As amphiregulin (Areg) has been implicated in lung homeostasis and repair upon neonatal pneumoniae (131) and its expression can also be controlled by NMU on type 2 cells (151), we also questioned whether *Areg* could be downregulated in severe infected pups. Gene expression analyses revealed no differences among groups (Figure 11C)

Considering that at this time point (P3), animals presenting severe disease are able to efficiently recruit neutrophils (Figure 8B), while also upregulating the *Cgrp* gene, it is tempting to speculate that the release of CGRP by sensory neurons could be supressing the conversion of neutrophils into the SiglecF^{hi} phenotype, and thus decreasing the bactericidal function of these cells and not directly their recruitment. With the decrease of *Vip* we would expect to observe a higher expression of pro-inflammatory cytokines, however almost no significative differences were found. Nonetheless, the expression of these cytokines is dependent on multiple factors, and these results may not be exclusively correlated.

3.5. GBS pneumonia severity linked to bacteria virulence

All the results described in the previous sections were performed using a hypervirulent strain of GBS belonging to the CC17. Finally, to determine whether the observed differences were exclusive of this strain and to model the disease in a less severe scenario, we last performed infections studies using a GBS strain that does not belong to the hypervirulent clone (non-CC17), the GBS NEM316 belonging to CC23. Using this strain, we evaluated the pups survival and their bacterial burden in the lung compared to those infected with the CC17 hypervirulent strain.

Compared with pups born from CC17-colonised mothers, the survival of pups born from non-CC17 progenitors was markedly increased (Figure 12A). The first and only death registered in non-CC17 infected animals was at P3 (~93.75%) (Figure 12A). None of the non-CC17 infected pups presented clinical signs of disease (data not shown). However, the bacterial load in the lung of pups infected with non-CC17 GBS did not show statistically significant differences when compared with the CC17 group (Figure 12B, left). Importantly, when CC17 pups were stratified by disease severity, we found similar bacterial burden between non-CC17 and CC17 infected pups presenting moderate disease, being both significatively decreased when compared with severe pups (Figure 12B, right).

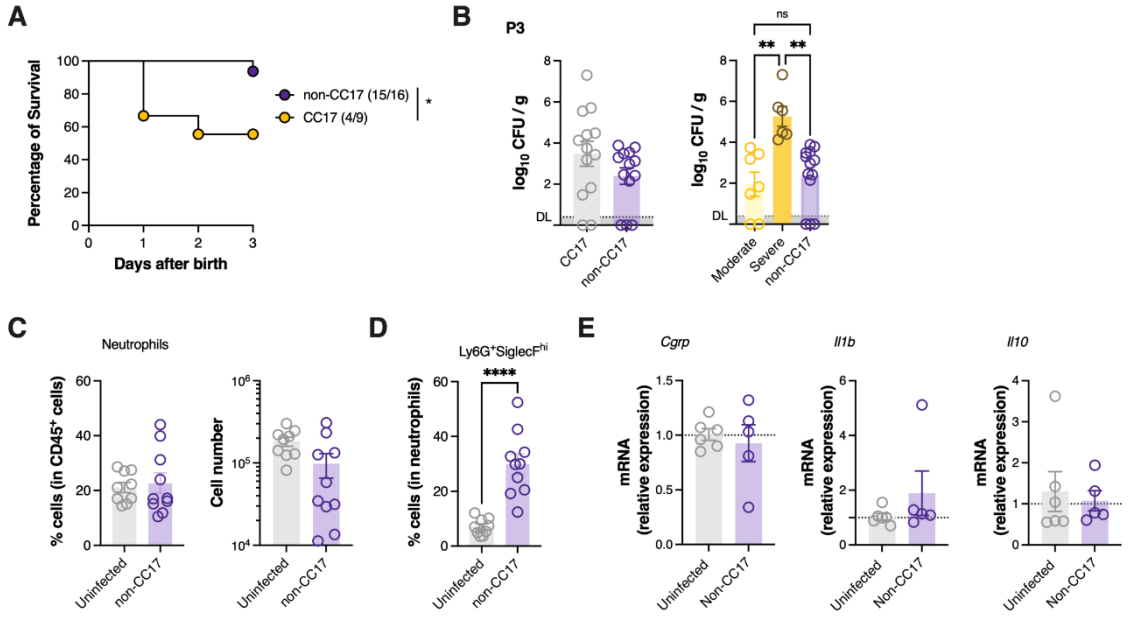

Figure 12. Infection study with a less virulent GBS strain. Pregnant C57BL/6 mice were intra-vaginally inoculated with 8x10^4 CFU of GBS hyper virulent strain BM110 (CC17) or the NEM316 strain (non-CC17) at gestational days 16 and 17. **(A)** Kaplan-Meier survival curve of neonatal mice born from GBS-colonised dams, monitored during a 3 days' period. The numbers in parentheses represent the number of animals that survived versus the total number of animals born. **(B)** Newborn mice were sacrificed at postnatal day 3 and the lung bacterial loads in the lung were determined. Data was also stratified by disease severity. Data are presented as mean ± SEM [n=17 (CC17); n=13 (non-CC17); n=7 (CC17 moderate); n= 6 (CC17 severe)]. **(C)** Frequency and number of neutrophils in the lung. Data are presented as mean ± SEM [n=9 (uninfected); n=10 (non-CC17)] **(D)** Frequency of Ly6G$^+$SiglecF^{hi} neutrophils in the lung. Data are presented as mean ± SEM [n=9 (uninfected); n=10 (non-CC17)] **(E)** Relative expression of the indicated genes analysed by RT-qPCR and normalized for the reference gene *Hprt* Data are presented as mean ± SEM [n=6 (uninfected); n=5 (non-CC17)]. Each symbol indicates data from single pup. Comparisons by one-way ANOVA or Student's *t*-test. Statistical differences (P values) between groups are indicated. * P < 0.05; ** P <0.1; *** P < 0.001; **** P < 0.0001; ns – Not significant.

Next, we further investigated if these animals would also present increased neutrophils in the lung, as previously observed with the CC17 strain (Figure 4C). Notably, no differences were observed in both the percentage and number of neutrophils in the lung of uninfected and non-CC17 infected pups (Figure 12C). However, a significant increase was found in the frequency of SiglecF^{hi} neutrophils (Figure 12D), similarly with the results obtained from animals infected with the virulent strain, that presented

moderate disease (Figure 8E). Consistently with our previous results in animals with moderate disease infected with the CC17 hypervirulent strain, non-CC17 infected pups did not present altered relative gene expression of *Cgrp*, *Il1b* and *Il10*, compared with control group (Figure 12E).

We conclude this study with the determination of relative expression of *CGRP*, *Il1b* and *Il10*, compared with control group (Figure 12E).

Altogether, our results support that higher severity in GBS pneumonia might be linked to the bacteria ability to evade the host immune system by inhibiting neutrophil activation, which in turn could impair the control of infection. Based on our findings, we hypothesized that GBS hijack the neuro-immune axis by leading to high expression of CGRP with concomitant inhibition of neutrophil activation. Nevertheless, we cannot disregard that CGRP upregulation could be a regulatory mechanism contributing to immunosuppression aiming at controlling excessive inflammation. On the other hand, immunosuppression can diminish effective and protective antibacterial immunity, thereby increasing susceptibility, as we have already described in a mouse model of GBS neonatal sepsis (104). This mechanism is currently being explored by our group. Namely, we are performing experiments in which CGRP signalling is blocked to assess whether neonates have increased survival, decreased bacterial load and higher neutrophil activation.

Conclusion

In conclusion, in this dissertation, we were able to adapt our BALB/c neonatal mouse model of GBS pneumonia to the C57BL/6 mice and characterise it. We showed that infected animals suffer lung alterations consistent with pneumonia that appear to leave respiratory sequels. Moreover, we found that infection leads to efficient recruitment of neutrophils, regardless of disease severity and outcome. Furthermore, although the numbers of γδ T cells also increase in the lung during neonatal pneumonia, these cells do not appear to have a protective decisive role in the acute phase of GBS infection. Nevertheless, this first encounter with the bacteria leads to higher frequency of a tissue-resident profile after the resolution of infection, indicating a possibility of a more effective response to a secondary challenge. Deeper analyses of the lung neutrophils phenotype during neonatal pneumonia suggest that the severity of GBS pneumonia might be connect with the capacity to recruit and activate neutrophils, displayed by the profile of high expression of SiglecF. Furthermore, severe disease was accompanied by the upregulation of the neuropeptide GCRP, a neuropeptide produced by nociceptor neurons that has already been described to impact neutrophil recruitment in other bacterial infection models. Here, although no differences were found in total neutrophil numbers between pups with different severity, we hypothesise that CGRP could impact neutrophil activation inhibiting the development of a more phagocytic profile, and thus establishing a possible relation of the neuro-immune axis in the capacity of GBS to the evade the host immune system (Figure 13).

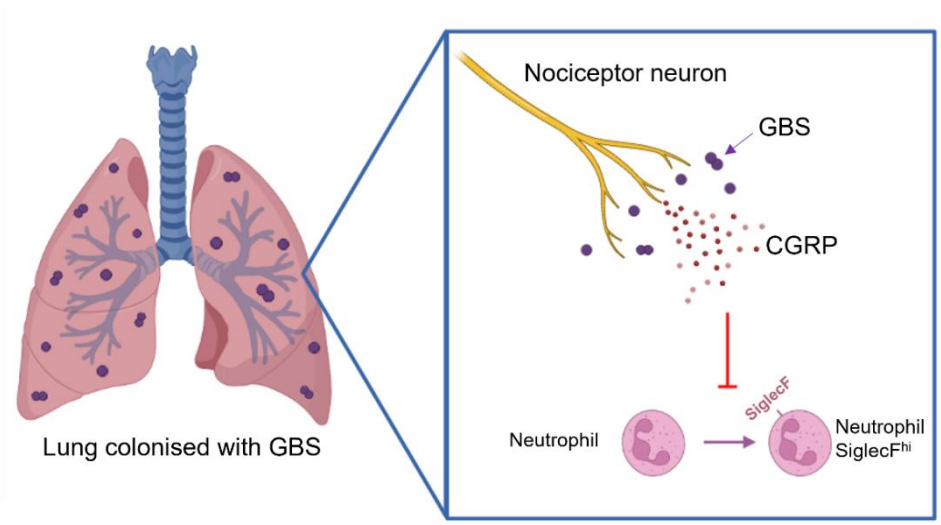

Figure 13. Schematic representation of a proposed mechanism by which GBS hijack the neuro-immune axis to evade the host innate immune system. GBS might interact and activate nociceptor neurons in the lung, which releases the neuropeptide CGRP. CGRP appears to hinder neutrophil activation into SiglecFhi neutrophil, a profile associated with increased bacterial clearance. Figure created in Biorender.

References

1. Anonymous,Prevention of Group B Streptococcal Early-Onset Disease in Newborns: ACOG Committee Opinion, Number 797. *Obstetrics & Gynecology* **135**, e51-e72 (2020).
2. T. M. Randis, J. A. Baker, A. J. Ratner, Group B Streptococcal Infections. *Pediatrics In Review* **38**, 254-262 (2017).
3. L. C. Paoletti, D. L. Kasper, Surface Structures of Group B *Streptococcus* Important in Human Immunity. *Microbiology Spectrum* **7** (2019).
4. C. B. Wilson, V. Nizet, Y. A. Maldonado, J. S. Remington, J. O. Klein, *Remington and Klein's Infectious Diseases of the Fetus and Newborn Infant* (Saunders Elsevier, Philadelphia ed. 8th, 2016).
5. J. Hall *et al.*, Maternal Disease With Group B *Streptococcus* and Serotype Distribution Worldwide: Systematic Review and Meta-analyses. *Clinical Infectious Diseases* **65**, S112-s124 (2017).
6. P. Sendi, L. Johansson, A. Norrby-Teglund, Invasive group B Streptococcal disease in non-pregnant adults : a review with emphasis on skin and soft-tissue infections. *Infection* **36**, 100-111 (2008).
7. L. Madrid *et al.*, Infant Group B Streptococcal Disease Incidence and Serotypes Worldwide: Systematic Review and Meta-analyses. *Clinical Infectious Diseases* **65**, S160-s172 (2017).
8. A. C. Seale *et al.*, Estimates of the Burden of Group B Streptococcal Disease Worldwide for Pregnant Women, Stillbirths, and Children. *Clinical Infectious Diseases* **65**, S200-S219 (2017).
9. K. Le Doare, P. T. Heath, An overview of global GBS epidemiology. *Vaccine* **31**, D7-D12 (2013).
10. J. Vornhagen, K. M. Adams Waldorf, L. Rajagopal, Perinatal Group B Streptococcal Infections: Virulence Factors, Immunity, and Prevention Strategies. *Trends in Microbiology* **25**, 919-931 (2017).
11. A. Berardi *et al.*, Understanding Factors in Group B *Streptococcus* Late-Onset Disease. *Infection and Drug Resistance* **14**, 3207-3218 (2021).
12. K. M. Edmond *et al.*, Group B streptococcal disease in infants aged younger than 3 months: systematic review and meta-analysis. *The Lancet* **379**, 547-556 (2012).
13. B. J. Stoll *et al.*, Early onset neonatal sepsis: the burden of group B Streptococcal and E. coli disease continues. *Pediatrics* **127**, 817-826 (2011).
14. H. C. Slotved, F. Kong, L. Lambertsen, S. Sauer, G. L. Gilbert, Serotype IX, a Proposed New *Streptococcus agalactiae* Serotype. *Journal of Clinical Microbiol*ogy **45**, 2929-2936 (2007).
15. S. Shabayek, B. Spellerberg, Group B Streptococcal Colonization, Molecular Characteristics, and Epidemiology. *Frontiers in Microbiology* **9** (2018).
16. A. Alhhazmi, G. J. Tyrrell, Phenotypic and molecular analysis of nontypeable Group B streptococci: identification of cps2a and hybrid cps2a/cps5 Group B streptococcal capsule gene clusters. *Emerging Microbes & Infections* **7**, 1-12 (2018).
17. N. Jones *et al.*, Multilocus Sequence Typing System for Group B *Streptococcus*. *Journal of Clinical Microbiol*ogy **41**, 2530-2536 (2003).
18. Q. Cheng *et al.*, Immunization with C5a peptidase or peptidase-type III polysaccharide conjugate vaccines enhances clearance of group B Streptococci from lungs of infected mice. *Infection and Immunity* **70**, 6409-6415 (2002).
19. A. L. Jones, R. H. Mertz, D. J. Carl, C. E. Rubens, A streptococcal penicillin-binding protein is critical for resisting innate airway defenses in the neonatal lung. *The Journal of Immunology* **179**, 3196-3202 (2007).

20. M. J. Baron, D. J. Filman, G. A. Prophete, J. M. Hogle, L. C. Madoff, Identification of a glycosaminoglycan binding region of the alpha C protein that mediates entry of group B Streptococci into host cells. *Journal of Biological Chemistry* **282**, 10526-10536 (2007).
21. G. R. Bolduc, L. C. Madoff, The group B streptococcal alpha C protein binds alpha1beta1-integrin through a novel KTD motif that promotes internalization of GBS within human epithelial cells. *Microbiology (Reading)* **153**, 4039-4049 (2007).
22. E. B. Andrade *et al.*, A mouse model reproducing the pathophysiology of neonatal group B streptococcal infection. *Nature Communications* **9**, 3138 (2018).
23. J. Koo, T. Escajadillo, L. Zhang, V. Nizet, S. M. Lawrence, Erythrocyte-Coated Nanoparticles Block Cytotoxic Effects of Group B *Streptococcus* β-Hemolysin/Cytolysin. *Front Pediatr* **7**, 410 (2019).
24. R. M. McAdams *et al.*, Choriodecidual Group B Streptococcal Infection Induces miR-155-5p in the Fetal Lung in *Macaca nemestrina*. *Infection and Immunity* **83**, 3909-3917 (2015).
25. J. B. Johnnidis *et al.*, Regulation of progenitor cell proliferation and granulocyte function by microRNA-223. *Nature* **451**, 1125-1129 (2008).
26. M. Deny, M. Romano, O. Denis, G. Casimir, M. Chamekh, Progressive Control of *Streptococcus agalactiae*-Induced Innate Inflammatory Response Is Associated with Time Course Expression of MicroRNA-223 by Neutrophils. *Infection and Immunity* **88** (2020).
27. S. A. Nanduri *et al.*, Epidemiology of Invasive Early-Onset and Late-Onset Group B Streptococcal Disease in the United States, 2006 to 2015: Multistate Laboratory and Population-Based Surveillance. *JAMA Pediatrics* **173**, 224-233 (2019).
28. Q. Cheng *et al.*, Antibody against surface-bound C5a peptidase is opsonic and initiates macrophage killing of group B streptococci. *Infection and Immunity* **69**, 2302-2308 (2001).
29. C. Tirone *et al.*, Gut and Lung Microbiota in Preterm Infants: Immunological Modulation and Implication in Neonatal Outcomes. *Frontiers in Immunology* **10**, 2910 (2019).
30. S. J. Schrag, J. R. Verani, Intrapartum antibiotic prophylaxis for the prevention of perinatal group B streptococcal disease: experience in the United States and implications for a potential group B streptococcal vaccine. *Vaccine* **31**, D20-D26 (2013).
31. M. B. Dhudasia, D. D. Flannery, M. R. Pfeifer, K. M. Puopolo, Updated guidance: prevention and management of perinatal group B *Streptococcus* infection. *NeoReviews* **22**, e177-e188 (2021).
32. R. K. Bouhafs, C. Jarstrand, B. Robertson, Lipid peroxidation of lung surfactant in experimental neonatal group B streptococcal pneumonia. *Lung* **182**, 61-72 (2004).
33. Y. Xu, Y. Dong, X. Guo, B. Sun, Suppression of pulmonary group B streptococcal proliferation and translocation by surfactants in ventilated near-term newborn rabbits. *Pediatric Research* **86**, 208-215 (2019).
34. V. M. Ranieri *et al.*, Acute respiratory distress syndrome: the Berlin Definition. *Jama* **307**, 2526-2533 (2012).
35. K. Y. Lee, Pneumonia, Acute Respiratory Distress Syndrome, and Early Immune-Modulator Therapy. *International Journal of Molecular Sciences* **18** (2017).
36. Anonymous, Pediatric acute respiratory distress syndrome: consensus recommendations from the Pediatric Acute Lung Injury Consensus Conference. *Pediatric Critical Care Medicine* **16**, 428-439 (2015).
37. L. F. Donnelly, *Fundamentals of pediatric imaging* (Academic Press, 2017).
38. K. S. Doran, V. Nizet, Molecular pathogenesis of neonatal group B streptococcal infection: no longer in its infancy. *Molecular Microbioogyl* **54**, 23-31 (2004).

39. V. G. Hemming, D. W. McCloskey, H. R. Hill, Pneumonia in the neonate associated with group B streptococcal septicemia. *American journal of diseases of children* **130**, 1231-1233 (1976).
40. R. Libster *et al.*, Long-term outcomes of group B streptococcal meningitis. *Pediatrics* **130**, e8-15 (2012).
41. E. Horváth-Puhó *et al.*, Mortality, neurodevelopmental impairments, and economic outcomes after invasive group B streptococcal disease in early infancy in Denmark and the Netherlands: a national matched cohort study. *The Lancet Child & Adolescent Health* **5**, 398-407 (2021).
42. A. Ma, L. A. Thompson, T. Corsiatto, D. Hurteau, G. J. Tyrrell, Epidemiological Characterization of Group B *Streptococcus* Infections in Alberta, Canada: An Update from 2014 to 2020. *Microbiology Spectrum* **9**, e0128321 (2021).
43. K.-Q. Kam *et al.*, Serotype distribution and incidence of invasive early onset and late onset group B streptococcal disease amongst infants in Singapore. *BMC Infectious Diseases* **21**, 1221 (2021).
44. A. K. Abbas, A. H. Lichtman, S. Pillai, *Cellular and molecular immunology* (Elsevier Health Sciences, 2021).
45. H. Kawamoto, N. Minato, Myeloid cells. *The International Journal of Biochemistry & Cell Biology* **36**, 1374-1379 (2004).
46. R. Bals, Epithelial antimicrobial peptides in host defense against infection. *Respiratory Research* **1**, 141-150 (2000).
47. S. McComb, A. Thiriot, B. Akache, L. Krishnan, F. Stark, Introduction to the Immune System.*Methods in Molecular Biology* **2024**, 1-24 (2019).
48. P. F. Zipfel, Complement and immune defense: from innate immunity to human diseases. *Immunology Letters* **126**, 1-7 (2009).
49. B. P. Kaur, E. Secord, Innate Immunity. *Immunology and Allergy Clinics of North America* **41**, 535-541 (2021).
50. S. W. Brubaker, K. S. Bonham, I. Zanoni, J. C. Kagan, Innate immune pattern recognition: a cell biological perspective. *Annual Review of Immunology* **33**, 257-290 (2015).
51. G. P. Amarante-Mendes *et al.*, Pattern Recognition Receptors and the Host Cell Death Molecular Machinery. *Frontiers in Immunology* **9**, 2379 (2018).
52. M. R. Sarrias *et al.*, The Scavenger Receptor Cysteine-Rich (SRCR) domain: an ancient and highly conserved protein module of the innate immune system. *Critical Reviews in Immunology* **24**, 1-37 (2004).
53. A. S. Akhade, N. Subramanian, "Cytoplasmic Sensing in Innate Immunity" in Reference Module in Life Sciences. (Elsevier, 2022), https://doi.org/10.1016/B978-0-12-821618-7.00012-2.
54. A. M. Kvarnhammar, L. O. Cardell, Pattern-recognition receptors in human eosinophils. *Immunology* **136**, 11-20 (2012).
55. S. Basha, N. Surendran, M. Pichichero, Immune responses in neonates. *Expert Review of Clinical Immunology* **10**, 1171-1184 (2014).
56. T. R. Kollmann, B. Kampmann, S. K. Mazmanian, A. Marchant, O. Levy, Protecting the Newborn and Young Infant from Infectious Diseases: Lessons from Immune Ontogeny. *Immunity* **46**, 350-363 (2017).
57. J. M. Koenig, M. C. Yoder, Neonatal neutrophils: the good, the bad, and the ugly. *Clinics Perinatology* **31**, 39-51 (2004).
58. G. L. Burn, A. Foti, G. Marsman, D. F. Patel, A. Zychlinsky, The Neutrophil. *Immunity* **54**, 1377-1391 (2021).
59. K. Li *et al.*, Age-dependent changes of total and differential white blood cell counts in children. *Chinese Medical Journal (Engl)* **133**, 1900-1907 (2020).
60. E. Pérez-Figueroa, P. Álvarez-Carrasco, E. Ortega, C. Maldonado-Bernal, Neutrophils: Many Ways to Die. *Frontiers in Immunology* **12**, 631821 (2021).
61. B. Rada, Neutrophil Extracellular Traps.Methods in *Molecular Biology* **1982**, 517-528 (2019).

62. C. Rosales, Neutrophils at the crossroads of innate and adaptive immunity. *Journal of Leukocyte Biology* **108**, 377-396 (2020).
63. M. A. Cassatella, N. K. Östberg, N. Tamassia, O. Soehnlein, Biological Roles of Neutrophil-Derived Granule Proteins and Cytokines. *Trends in Immunolgy* **40**, 648-664 (2019).
64. S. Chirumbolo, G. Bjørklund, A. Sboarina, A. Vella, The role of basophils as innate immune regulatory cells in allergy and immunotherapy. *Human Vaccines & Immunotherapeutics* **14**, 815-831 (2018).
65. C. Nakashima, A. Otsuka, K. Kabashima, Recent advancement in the mechanism of basophil activation. *Journal of Dermatological Science* **91**, 3-8 (2018).
66. M. E. Rothenberg, S. P. Hogan, The eosinophil. *Annual Review of Immunology* **24**, 147-174 (2006).
67. K. A. Ravin, M. Loy, The Eosinophil in Infection. *Clinical Reviews in Allergy & Immunology* **50**, 214-227 (2016).
68. P. F. Weller, L. A. Spencer, Functions of tissue-resident eosinophils. *Nature Reviews Immunology* **17**, 746-760 (2017).
69. Y. Yamanishi, H. Karasuyama, Basophil-derived IL-4 plays versatile roles in immunity. *Seminars in Immunopathology* **38**, 615-622 (2016).
70. M. Dhakal, M. M. Miller, A. A. Zaghouani, M. P. Sherman, H. Zaghouani, Neonatal Basophils Stifle the Function of Early-Life Dendritic Cells To Curtail Th1 Immunity in Newborn Mice. *Journal of Immunology***195**, 507-518 (2015).
71. M. J. Butcher, J. Zhu, Recent advances in understanding the Th1/Th2 effector choice. *Fac Rev* **10**, 30 (2021).
72. A. Manoura *et al.*, Eosinophilia in sick neonates. *Haematologia (Budap)* **32**, 31-37 (2002).
73. A. Ardain, M. J. Marakalala, A. Leslie, Tissue-resident innate immunity in the lung. *Immunology* **159**, 245-256 (2020).
74. M. Guilliams, G. R. Thierry, J. Bonnardel, M. Bajenoff, Establishment and Maintenance of the Macrophage Niche. *Immunity* **52**, 434-451 (2020).
75. L. van de Laar *et al.*, Yolk Sac Macrophages, Fetal Liver, and Adult Monocytes Can Colonize an Empty Niche and Develop into Functional Tissue-Resident Macrophages. *Immunity* **44**, 755-768 (2016).
76. S. C. Funes, M. Rios, J. Escobar-Vera, A. M. Kalergis, Implications of macrophage polarization in autoimmunity. *Immunology* **154**, 186-195 (2018).
77. R. M. Steinman, H. Hemmi, Dendritic cells: translating innate to adaptive immunity. *Current Topics in Microbiology and Immunology* **311**, 17-58 (2006).
78. S. Ygberg, A. Nilsson, The developing immune system - from foetus to toddler. *Acta Paediatrica* **101**, 120-127 (2012).
79. S. J. Lalor, R. M. McLoughlin, Memory γδ T Cells-Newly Appreciated Protagonists in Infection and Immunity. *Trends in Immunology* **37**, 690-702 (2016).
80. C. Khairallah, T. H. Chu, B. S. Sheridan, Tissue Adaptations of Memory and Tissue-Resident Gamma Delta T Cells. *Frontiers in Immunology* **9**, 2636 (2018).
81. M. Papadopoulou, G. Sanchez Sanchez, D. Vermijlen, Innate and adaptive γδ T cells: How, when, and why. *Immunological Reviews* **298**, 99-116 (2020).
82. A. Voisin, F. Saez, J. R. Drevet, R. Guiton, The epididymal immune balance: a key to preserving male fertility. *Asian Journal of Andrology* **21**, 531-539 (2019).
83. D. Yüzen, P. C. Arck, K. Thiele, Tissue-resident immunity in the female and male reproductive tract. *Seminars in Immunopathology* 10.1007/s00281-022-00934-8 (2022).
84. R. L. Gallo, L. V. Hooper, Epithelial antimicrobial defence of the skin and intestine. *Nature Reviews Immunology* **12**, 503-516 (2012).
85. M. Kim *et al.*, Bacterial Interactions with the Host Epithelium. *Cell Host & Microbe* **8**, 20-35 (2010).

86. Y. Belkaid, T. W. Hand, Role of the microbiota in immunity and inflammation. *Cell* **157**, 121-141 (2014).
87. Ivanov, II, T. Tuganbaev, A. N. Skelly, K. Honda, T Cell Responses to the Microbiota. *Annual Review of Immunology***40**, 559-587 (2022).
88. M. Cheng, S. Hu, Lung-resident γδ T cells and their roles in lung diseases. *Immunology* **151**, 375-384 (2017).
89. C. E. Rubens, S. Smith, M. Hulse, E. Y. Chi, G. van Belle, Respiratory epithelial cell invasion by group B streptococci. *Infection and Immunity* **60**, 5157-5163 (1992).
90. G. V. De Gaetano *et al.*, The Streptococcus agalactiae cell wall-anchored protein PbsP mediates adhesion to and invasion of epithelial cells by exploiting the host vitronectin/α(v) integrin axis. *Molecular Microbiology* **110**, 82-94 (2018).
91. L. Sharma, J. Feng, C. J. Britto, C. S. Dela Cruz, Mechanisms of Epithelial Immunity Evasion by Respiratory Bacterial Pathogens. *Frontiers in Immunology* **11**, 91 (2020).
92. T. D. Starner, B. Agerberth, G. H. Gudmundsson, P. B. McCray, Expression and Activity of β-Defensins and LL-37 in the Developing Human Lung. *The Journal of Immunology* **174**, 1608-1615 (2005).
93. R. A. Dorschner, K. H. Lin, M. Murakami, R. L. Gallo, Neonatal Skin in Mice and Humans Expresses Increased Levels of Antimicrobial Peptides: Innate Immunity During Development of the Adaptive Response. *Pediatric Research* **53**, 566-572 (2003).
94. A. Borghesi, M. Stronati, J. Fellay, Neonatal Group B Streptococcal Disease in Otherwise Healthy Infants: Failure of Specific Neonatal Immune Responses. *Frontiers in Immunology***8**, 215 (2017).
95. K. H. Restori, B. T. Srinivasa, B. J. Ward, E. D. Fixman, Neonatal Immunity, Respiratory Virus Infections, and the Development of Asthma. *Frontiers in Immunology* **9**, 1249 (2018).
96. G. Mancuso *et al.*, Role of interleukin 12 in experimental neonatal sepsis caused by group B streptococci. *Infection and Immunity* **65**, 3731-3735 (1997).
97. C. Biondo *et al.*, Essential Role of Interleukin-1 Signaling in Host Defenses Against Group B Streptococcus. *mBio* **5**, e01428-01414 (2014).
98. K. Upadhyay *et al.*, Group B Streptococci Induce Proinflammatory Responses via a Protein Kinase D1-Dependent Pathway. *Journal of Immunology* **198**, 4448-4457 (2017).
99. N. Mohammadi *et al.*, Neutrophils Directly Recognize Group B Streptococci and Contribute to Interleukin-1β Production during Infection. *PLoS One* **11**, e0160249 (2016).
100. R. Feuerstein *et al.*, Macrophages Are a Potent Source of *Streptococcus*-Induced IFN-β. *Journal of Immunology* **203**, 3416-3426 (2019).
101. E. Movert *et al.*, Secreted group IIA phospholipase A2 protects humans against the group B *Streptococcus*: experimental and clinical evidence. *The Journal of Infectious Diseases* **208**, 2025-2035 (2013).
102. A. Costa *et al.*, Activation of the NLRP3 Inflammasome by Group B Streptococci. *The Journal of Immunology* **188**, 1953-1960 (2012).
103. D. Clarke *et al.*, Group B *Streptococcus* Induces a Robust IFN-γ Response by CD4(+) T Cells in an In Vitro and In Vivo Model. Journal of Immunology Research **2016**, 5290604 (2016).
104. E. B. Andrade *et al.*, TLR2-induced IL-10 production impairs neutrophil recruitment to infected tissues during neonatal bacterial sepsis. *Journal of Immunology* **191**, 4759-4768 (2013).
105. M. Bebien *et al.*, The pore-forming toxin β hemolysin/cytolysin triggers p38 MAPK-dependent IL-10 production in macrophages and inhibits innate immunity. *PLoS Pathogens* **8**, e1002812 (2012).

106. S. L. Kolar *et al.*, Group B *Streptococcus* Evades Host Immunity by Degrading Hyaluronan. *Cell Host Microbe* **18**, 694-704 (2015).
107. J. H. Reynolds, G. McDonald, H. Alton, S. B. Gordon, Pneumonia in the immunocompetent patient. *The British Journal of Radiology* **83**, 998-1009 (2010).
108. B. Périchon *et al.*, Regulation of PI-2b Pilus Expression in Hypervirulent *Streptococcus agalactiae* ST-17 BM110. *PloS one* **12**, e0169840-e0169840 (2017).
109. F.-Y. C. Lin *et al.*, Phylogenetic lineages of invasive and colonizing strains of serotype III group B Streptococci from neonates: a multicenter prospective study. *Journal of Clinical Microbiology* **44**, 1257-1261 (2006).
110. M. Buscetta *et al.*, PbsP, a cell wall-anchored protein that binds plasminogen to promote hematogenous dissemination of group B *Streptococcus*. *Molecular Microbiology* **101**, 27-41 (2016).
111. M. Canzian *et al.*, SEMIQUANTITATIVE ASSESSMENT OF SURGICAL LUNG BIOPSY: PREDICTIVE VALUE AND IMPACT ON SURVIVAL OF PATIENTS WITH DIFFUSE PULMONARY INFILTRATE. *Clinics* **62**, 23-30 (2007).
112. F. A. Pinho-Ribeiro *et al.*, Blocking Neuronal Signaling to Immune Cells Treats Streptococcal Invasive Infection. *Cell* **173**, 1083-1097.e1022 (2018).
113. P. Baral *et al.*, Nociceptor sensory neurons suppress neutrophil and γδ T cell responses in bacterial lung infections and lethal pneumonia. *Nature Medicine* **24**, 417-426 (2018).
114. R. M. McAdams *et al.*, Choriodecidual infection downregulates angiogenesis and morphogenesis pathways in fetal lungs from *Macaca nemestrina*. PLoS One. 2012;7(10):e46863.
115. B. Fehlhaber *et al.*, A sensitive scoring system for the longitudinal clinical evaluation and prediction of lethal disease outcomes in newborn mice. *Scientific Reports* **9**, 5919 (2019).
116. A. Torres *et al.*, Pneumonia. *Nature Reviews Disease Primers* **7**, 25 (2021).
117. J. H. Vollman, W. L. Smith, E. T. Ballard, I. J. Light, Early onset group B streptococcal disease: Clinical, roentgenographic, and pathologic features. *The Journal of Pediatrics* **89**, 199-203 (1976).
118. C. E. Rubens *et al.*, Pathophysiology and histopathology of group B streptococcal sepsis in *Macaca nemestrina* primates induced after intraamniotic inoculation: evidence for bacterial cellular invasion. *The Journal of Infectious Diseases* **164**, 320-330 (1991).
119. P. Madureira *et al.*, Inhibition of IL-10 Production by Maternal Antibodies against Group B *Streptococcus* GAPDH Confers Immunity to Offspring by Favoring Neutrophil Recruitment. *PLoS Pathogensens* **7**, e1002363 (2011).
120. I. M. de Kleer *et al.*, Perinatal Activation of the Interleukin-33 Pathway Promotes Type 2 Immunity in the Developing Lung. *Immunity* **45**, 1285-1298 (2016).
121. Z. Sun *et al.*, Fpr2/CXCL1/2 Controls Rapid Neutrophil Infiltration to Inhibit *Streptococcus agalactiae* Infection. *Frontiers in Immunology* **12**, 786602 (2021).
122. C. Biondo *et al.*, The interleukin-1β/CXCL1/2/neutrophil axis mediates host protection against group B streptococcal infection. Infection and Immunity **82**, 4508-4517 (2014).
123. C. Nathan, Neutrophils and immunity: challenges and opportunities. *Nature Reviews Immunology* **6**, 173-182 (2006).
124. B. Wonnenberg *et al.*, IL-17A attracts inflammatory cells in murine lung infection with *P. aeruginosa*. *Innate Immunity* **22**, 620-625 (2016).
125. L. Borkner, L. M. Curham, M. M. Wilk, B. Moran, K. H. G. Mills, IL-17 mediates protective immunity against nasal infection with *Bordetella pertussis* by mobilizing neutrophils, especially Siglec-F(+) neutrophils. *Mucosal Immunol*ogy **14**, 1183-1202 (2021).

126. S. Qiao *et al.*, Endogenous IL-17A mediated neutrophil infiltration by promoting chemokines expression during chlamydial lung infection. *Microbial Pathogenesis* **129**, 106-111 (2019).
127. A. K. Wright *et al.*, Experimental human pneumococcal carriage augments IL-17A-dependent T-cell defence of the lung. *PLoS Pathogens* **9**, e1003274 (2013).
128. P. L. Simonian *et al.*, IL-17A-expressing T cells are essential for bacterial clearance in a murine model of hypersensitivity pneumonitis. *Journal of Immunology* **182**, 6540-6549 (2009).
129. R. Muro, H. Takayanagi, T. Nitta, T cell receptor signaling for γδT cell development. *Inflammation and Regeneration* **39**, 6 (2019).
130. M. E. Parker, M. Ciofani, Regulation of γδ T Cell Effector Diversification in the Thymus. *Frontiers in Immunology* **11** (2020).
131. J. G. Xi-zhi *et al.*, Lung γδ T cells mediate protective responses during neonatal influenza infection that are associated with type 2 immunity. *Immunity* **49**, 531-544. e536 (2018).
132. V. Bronte, M. J. Pittet, The spleen in local and systemic regulation of immunity. *Immunity* **39**, 806-818 (2013).
133. A. G. Murphy *et al.*, *Staphylococcus aureus* infection of mice expands a population of memory γδ T cells that are protective against subsequent infection. *Journal of Immunology* **192**, 3697-3708 (2014).
134. J. C. Ribot, N. Lopes, B. Silva-Santos, γδ T cells in tissue physiology and surveillance. *Nature Reviews Immunology* **21**, 221-232 (2021).
135. S. F. Ziegler, F. Ramsdell, M. R. Alderson, The activation antigen CD69. *Stem Cells* **12**, 456-465 (1996).
136. D. Cibrián, F. Sánchez-Madrid, CD69: from activation marker to metabolic gatekeeper. *European Journal of Immunologyl* **47**, 946-953 (2017).
137. R. C. Budd *et al.*, Distinction of virgin and memory T lymphocytes. Stable acquisition of the Pgp-1 glycoprotein concomitant with antigenic stimulation. *Journal of Immunology* **138**, 3120-3129 (1987).
138. K. Kelly, K. Shortman, R. Scollay, The surface phenotype of activated T lymphocytes. *Immunology and Cell Biology* **66**, 297-306 (1988).
139. S. Huet *et al.*, CD44 contributes to T cell activation. *Journal of Immunology* **143**, 798-801 (1989).
140. S. L. Swain *et al.*, From naive to memory T cells. *Immunological Reviews* **150**, 143-167 (1996).
141. M. G. McHeyzer-Williams, M. M. Davis, Antigen-Specific Development of Primary and Memory T Cells in Vivo. *Science* **268**, 106-111 (1995).
142. H. Renz, C. Skevaki, Early life microbial exposures and allergy risks: opportunities for prevention. *Nature Reviews Immunology* **21**, 177-191 (2021).
143. A. C. Kirby, D. J. Newton, S. R. Carding, P. M. Kaye, Pulmonary dendritic cells and alveolar macrophages are regulated by gammadelta T cells during the resolution of *S. pneumoniae*-induced inflammation. *The Journal of Pathology* **212**, 29-37 (2007).
144. S. Ryu *et al.*, Siglec-F–expressing neutrophils are essential for creating a profibrotic microenvironment in renal fibrosis. *The Journal of Clinical Investigation* **132** (2022).
145. C. Engblom *et al.*, Osteoblasts remotely supply lung tumors with cancer-promoting SiglecF(high) neutrophils. *Science* **358** (2017).
146. D. M. Calcagno *et al.*, SiglecF(HI) Marks Late-Stage Neutrophils of the Infarcted Heart: A Single-Cell Transcriptomic Analysis of Neutrophil Diversification. *Journal of the American Heart Association* **10**, e019019 (2021).
147. C. Pfirschke *et al.*, Tumor-Promoting Ly-6G(+) SiglecF(high) Cells Are Mature and Long-Lived Neutrophils. *Cell Reports* **32**, 108164 (2020).
148. E. Vafadarnejad *et al.*, Dynamics of Cardiac Neutrophil Diversity in Murine Myocardial Infarction. *Circulation Research* **127**, e232-e249 (2020).

149. J. W. Shin *et al.*, A unique population of neutrophils generated by air pollutant-induced lung damage exacerbates airway inflammation. *The Journal of Allergy and Clinical Immunology* **149**, 1253-1269.e1258 (2022).
150. M. Schiller, T. L. Ben-Shaanan, A. Rolls, Neuronal regulation of immunity: why, how and where? *Nature Reviews Immunology* **21**, 20-36 (2021).
151. J. R. Huh, H. Veiga-Fernandes, Neuroimmune circuits in inter-organ communication. *Nature Reviews Immunology* **20**, 217-228 (2020).
152. V. Cardoso *et al.*, Neuronal regulation of type 2 innate lymphoid cells via neuromedin U. *Nature* **549**, 277-281 (2017).
153. A. Wallrapp *et al.*, The neuropeptide NMU amplifies ILC2-driven allergic lung inflammation. *Nature* **549**, 351-356 (2017).
154. D. Ganea, K. M. Hooper, W. Kong, The neuropeptide vasoactive intestinal peptide: direct effects on immune cells and involvement in inflammatory and autoimmune diseases. *Acta Physiologica (Oxf)* **213**, 442-452 (2015).